# Mooring Analysis of a Novel FSPV Plant in Offshore Environment (Public Version)


**Submitted on** 31 August 2020
**Submitted by** BADERIYA Naman
**Address:** Gayatri Traders, Krishna Nagar, Satna (M.P.) – 485001, India
**Email Address:** naman.baderiya@eleves.ec-nantes.fr
**Student ID No.:** 190610Z

**Supervisor:** Damian Villaverde Vega, International Marine and Dredging Consultancy


| | |
|---|---|
| EMship+ Advanced Design | *This Master Thesis has been prepared as part of the graduation of the Master in Marine Technology specialized in Hydrodynamics for Ocean Engineering from Centrale Nantes and the graduation of the double Master degree Liège University-Centrale Nantes in the EMship+ programme* |

# ABSTRACT

In the urge of increasing the harvest of renewable energy, solar floating PV plants are planned to install in offshore condition. It provides an advantage by increase the energy yield of the system compared to land-based systems as well it has the freedom to extend in the area without restriction or reduction in the solar irradiance. This research thesis covers the development of the FSPV plant in the offshore condition and proposes a novel design of the floaters for the same that can sustain in the open sea condition. Further, an optimised mooring layout is developed from a conventional one which is verified by the mooring analysis. Anchor selection for both systems is presented in the work. It also provides information about challenges faced while developing and modelling the design and finally, future researches are defined for the full development of the design.

# TABLE OF CONTENTS

# DECLARATION OF AUTHORSHIP

I declare that this thesis and the work presented in it are my own and have been generated by me as the result of my own original research.

Where I have consulted the published work of others, this is always clearly attributed.

Where I have quoted from the work of others, the source is always given. With the exception of such quotations, this thesis is entirely my own work.

I have acknowledged all main sources of help.

Where the thesis is based on work done by myself jointly with others, I have made clear exactly what was done by others and what I have contributed myself.

This thesis contains no material that has been submitted previously, in whole or in part, for the award of any other academic degree or diploma.

I cede copyright of the thesis in favour of the Ecole Centrale de Nantes.

Date: 31st August 2020 Signature:

# ACKNOWLEDGEMENTS

This thesis is the completion of the European Master course in Advanced Design in Ship and Offshore Structure at Universite de Liege/Ecole Centrale de Nantes. I could not have done it without the help and support of several people and I would like to thank them sincerely for their contributions.

First and foremost, I would like to thank my supervisor Damian Villaverde Vega, for his friendly, professional and insightful assistance.  He has been very helpful, especially providing the critical depth knowledge of the subject and guiding me throughout the process irrespective of his schedule.

Furthermore, I would like to thank Zafar Samadov and IMDC for providing me with such a great opportunity to work there and to gain professional experience.

I would also like to thank the blue energy team of IMDC, especially Lorenzo and Massimo who had extended there help for my doubts. I also like to thank the other members of IMDC especially Petra, Lesley and Gwen for making me feel comfortable in the company from the first day and helping me out with the administrative formalities and difficulties.

Lastly, I would like to thank EMShip coordinator, Professor Philippe Rigo and Professor Lionel Gentaz for giving me this auspicious chance for pursuing this master and providing me support and motivation throughout my master's journey.

# List of Figures

## List of Tables

# 1. INTRODUCTION

## 1.1. Project Background

Energy demand is growing, while the conventional resources are remaining limited. The issue of energy pricing, surging every moment with oil and gas markets, remains an unstable one. With the climate change issue in mind, the world is focusing more and more on clean, locally available and cost-efficient energy solutions such as those from renewable energy sources.

Solar is one of the best choices among all renewable energy sources. It is not as heavy in terms of the capital costs as tidal and geothermal (and much less risky); it is simple, but, unlike wind and waves, quite predictable. The change is already happening. From utility-scale grid-connected solar PV plants, solar-powered airports, railways, temples and cricket stadiums, to tiny villages with no electricity access, we are seeing cost-efficient and environmentally friendly solar power projects springing up everywhere.

With the increasing demand of solar energy generating capacity, floating solar PV plants provide new opportunities for scaling up solar energy generating capacity, specifically where high population density and land are the major constraints. Having the advantage of potentially better energy yield due to cooling effect of water and presence of low dust, floating solar PV plants are now dominating over ground-mounted PV plants in areas where the use of land and constructability are the major concerns.

Taking the floating solar PV plants to the offshore environment provides an additional benefit since its size is no more govern with the area available in the inland water bodies. Furthermore, the energy yield of the plant is amplified as going to offshore eliminates any chance of the sheltering effect of sunlight due to the shore structure that is present around the inland water bodies.

## 1.2. Scope of the Thesis

This thesis proposes a design for the floaters of floating solar PV (FSPV) plants that can sustain in the offshore condition. It is designed for the Hollandse Kust (Noord) wind farm zone (HKN). Furthermore, a hybrid mooring layout is presented for the plant to reduce the mooring footprint. The structure of the report is followed as:

- ***Chapter 1*:** This chapter serves as the introduction to the reader providing a brief background of the topic as well as giving information about the organization of the thesis.
- ***Chapter 2:*** This chapter provides detail about the different technologies for the FSPV plant that are used by the industries like floaters, mooring and anchoring.
- ***Chapter 3:*** This chapter gives the details about the site where the plant is planned to be installed as well as the environmental condition present at the site.
- ***Chapter 4:*** This chapter discusses the different design basis of the floaters and mooring system, based on it, designing of them is done
- ***Chapter 5:*** This chapter describes the design philosophy that has been considered. It further talks about the selection and a brief introduction to the software. It provides information about the factor of safety that has been used.
- ***Chapter 6:*** This chapter presents the conceptual design of the floaters and the mooting system.
- ***Chapter 7:*** This discusses the setup of the mooring system and also about the results of the analysis
- ***Chapter 8:*** This chapter presents the method and gives the information about the procedure for selecting the anchor as well as the final selected anchor.
- ***Chapter 9:*** This chapter gives a conclusion for the thesis.
- ***Chapter 10:*** This chapter suggests the different area on which future research has to be done.

# 2. TECHNOLOGICAL ASSESSMENT OF FSPV

This section gives the overview information about the technology used by the industry for the floaters, mooring and anchors.

## 2.1. Type of Floaters

FSPV system represents an emerging opportunity in which solar PV systems are installed directly on the water bodies, such as oceans, lakes, ponds, or reservoirs. Although FSPV plants are relatively a newer concept in the renewable energy in general, and solar in particular, landscape, many companies have designed systems and begin to establish a proven track record by deploying FSPV in the onshore environment. On the contrary, when it comes to the offshore environment, it is still in an early stage of designing since the concept of onshore cannot be used due to the harsh environmental conditional and other technical difficulties like high risk of corrosion due to saltwater and exposer of the inverter and Balance of system (BOS) components to the high humidity environments and movements due to the waves, etc. This condition leads to the development of a new concept for the offshore environment.

Besides floater design, there are other factors too that need to be taken care when designing it for the offshore conditions such as mooring system, PV module technology and electrical systems, material composition, tilt angle limitation of the modules, etc.

This section provides an overview of the different concepts that are being developed by the companies and research institutes for the open sea and near-shore environment. Since these concepts are in the developing phase, information for them are very limited.

#### *2.1.1.1. Zon op Zee (Solar-at-Sea)*

Zon op Zee project, shown in Figure 2-1, is developed by the consortium comprising of six Dutch companies and Research Organizations including TNO, MARIN, ONE-Dyas and Oceans of Energy. It is the first-ever offshore solar farm installed at open sea. It is a modular-based designed which can be easily expanded and are capable to withstand rough sea (upto 13 meters). In 2019, they had installed the first pilot project of 28 modules (8.5kW) in the Dutch North Sea for the testing which had been recently doubled to 56 modules (17kW) and had survived the winter storm including storm “Ciara”.

*Figure 2-1: Zon op Zee (Solar-at-Sea)*
*https://oceansofenergy.blue/wp-content/uploads/2020/01/20200129-OOE-offshore-floating-solar -farm-system-doubled-in-size_for-website.jpg*

#### ***2.1.1.2. HelioFloat***

HelioFloat offshore platform, shown in Figure 2-2, is developed by the HeliFloat, a company founded by the professors of Vienna University of Technology. It is still in the development phase and work is going on different prototypes in different scales to test all possible operation modes. These platforms are based on a pressure-based skirt system which is connected through a lightweight structure. Practically, the platform rests on a series of barrels to provide flotation and are made up of a soft, flexible material that is open to the sea at the bottom like the ballast tanks on a submarine. Air is trapped inside the floats and compressed by water pressure to act as a shock absorber. Whereas, the sides of the barrel flex as the waves strike them, so they absorb less energy than hard floats. Taken these two effects together, made it possible to withstand rough seas while remaining stable. Generally, the supporting air chambers are filled with a blower to lift the platform 10 to 15 meters above sea level. As collateral security conventional buoys are also fixed on the bottom of the floater.

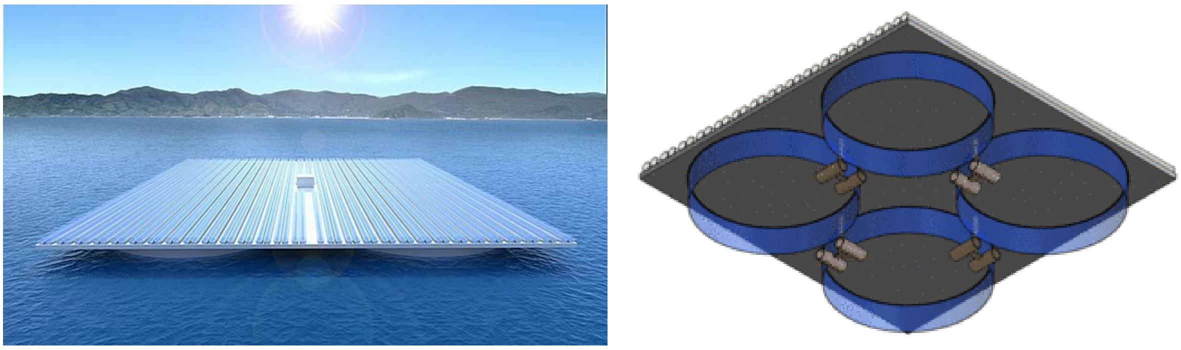

*Figure 2-2: HelioFloat Offshore Platform*
https://www.heliofloat.com/index.php?id=17

#### *2.1.1.3. Floating Solar Park*

Floating Solar Park, shown in Figure 2-3, is developed by Moss Maritime suitable for the onshore and offshore location. It is in the development phase. This design is also based on standardized modules (typically of 10*10m) that are specifically designed based on the location and weather. Each module consists of a platform on top where the solar panels are placed and this platform is supported by vertical columns which provide the required buoyancy and air gap. The modules are connected with a flexible connection to allow it to follow the wave slope. They are designed to withstand the swell waves with significant heights upto 3-4 m with long periods.

*Figure 2-3: Floating Solar Park*
https://www.norwep.com/content/download/34430/253411/version/1/file/Lars+Bjar+Moss+Maritime+v2.pdf

#### 2.1.1.4. SolarSea

SolarSea project, shown in Figure 2-4, is developed by the SwimSol with the help of the Vienna University of Technology. The floater is designed for the nearshore that can survive waves of tropical shallow-water lagoons (upto 1.5m), as well as the currents, tides, extreme UV, humidity and is corrosion-proof. The floater consists of a top part where solar modules are placed, supported by the column to provide the sufficient buoyancy and the air gap which can be seen in the second picture.

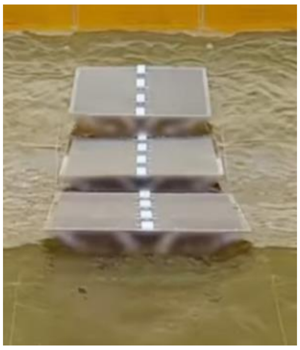

*Figure 2-4: SolarSea*
*https://swimsol.com/solar-projects/floating-photovoltaic-offshore-solar-sea-power-pv-four-seasons/*
*https://youtu.be/PMQbhmMIIVE?t=18*

#### 2.1.1.5. Ocean Sun

Figure 2-5 shows the floating solar plant designed by Ocean Sun. Their design is inspired by the aquaculture farm and suitable for the near-shore and semi-sheltered waters. In this design, the modules are installed on the double keder that are welded on the thin and flexible reinforced membrane. These membranes are hydro-elastic which allows the structure and the PV modules to move gracefully with the harmonics of the waves, as opposed to working against the forces from the waves. Furthermore, the thickness of the membrane is only 1mm which enables the panels to be in direct thermal contact with the water, that contributes significantly to heat dissipation and, as a result, the modules yield is improved. These membranes are further fixed with the buoyancy ring that provides the needed buoyancy to the system. The bilge pump is provided on the membrane for removing the water on the membrane due to the train.

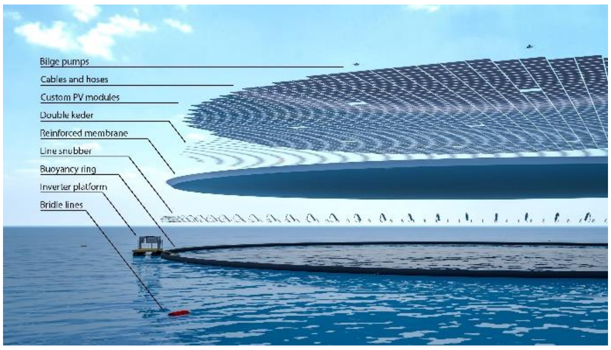

*Figure 2-5: Ocean Sun*
https://oceansun.no/wp-content/uploads/2020/03/Flytebrygge-med-tekst.jpg
https://oceansun.no/wp-content/uploads/2020/04/Skaftaa-midfjord.jpg

## 2.2. Mooring

The mooring system used for station keeping that maintains in keeping the plant in limited excursions and also limiting the acceleration of the plant. It is one of another important issue for the designing of FSPV plant. This section gives details about the different mooring layout and makeup of the mooring lines presently used in different industries.

### *2.2.1. Mooring Layout*

The layout of the mooring for the FSPV in the offshore environment can be inspired from the offshore oil platform and it is driven by the water depth, response of the structure in a wave, allowable excursion of the floater and the environmental condition. Further, it will govern the mooring makeup, material and the type of anchor used for the FSPV.

Broadly, the different configuration of the mooring layout for FSPV can be split into three categories as proposed by (Rosa-Clot and Tina, 2020): Catenary mooring system, Taut mooring system and hybrid mooring system. Although, the concepts proposed in the book by (Rosa-Clot and Tina, 2020) mainly focus for the rivers and near-shore environment but it can be taken as a fundamental building block or the starting point in designing of mooring system for the open sea and can be developed accordingly for the particular case. They also proposed a rigid mooring system which is not a feasible option for the open sea in terms of flexibility and cost associated with it.

#### 2.2.1.1. Catenary Mooring

This configuration got its name from the catenary shape that is formed by the mooring lines, shown in Figure 2-6. This system uses the self-weight and the friction of the line with the sea bed to generate the required restoring force. It requires a large segment of the line to lies on the sea bed which produces needed friction.

This system requires larger mooring footprint. It is relatively simple to install (depending on the anchoring). If drag anchors are used, then a settling distance is required to embed the anchor into the sea bed. It is not suitable to withstand vertical loads. However, this problem can be overcome by using intermediate buoys.

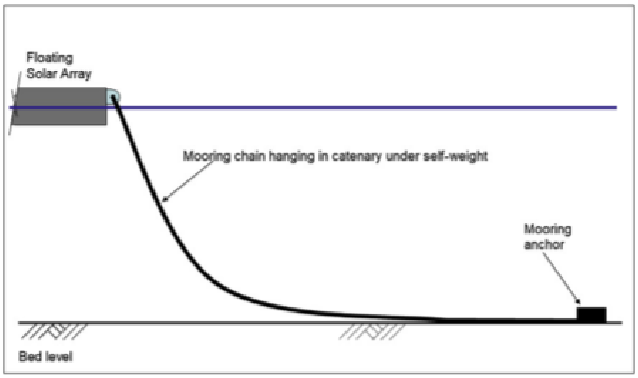


*Figure 2-6: Catenary Mooring System(Rosa-Clot and Tina, 2020)*

#### 2.2.1.2. Taut Mooring System

In this configuration, as the name justifies the mooring lines are connected until they are fully taut which is shown in Figure 2-7. This system creates the restoring forces from the line deformation rather than its weight, in other words, it is generated by the axial elastic stretching of the lines. In this system, lines are generally aligned vertically but it can also be inclined. This system only allows the limited movement of the floaters.

Drag anchors cannot be used for these kinds of mooring system as it required the anchors to be embedded in the sea bed to provide load-bearing capacity in both horizontal and vertical direction. It requires smaller mooring footprint.

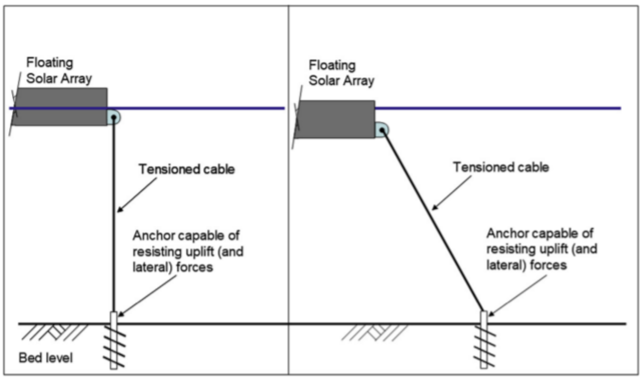


*Figure 2-7: Taut Mooring System(Rosa-Clot and Tina, 2020)*

### *2.2.1.3. Hybrid Mooring System*

In this mooring system, a weight or floater is added in the lines between the FSPV and the anchors, shown in Figure 2-8. This can have either catenary mooring characteristics or taut mooring characteristics. In Catenary mooring using of these additions largely reduce the mooring footprint. Clump weight/sinker provide additional support to the anchor to bear the load which make it possible to reduce the length of a line in catenary mooring while in taut mooring it provides the stiffness to the lines necessary with the variation in water level. Whereas similar principle applies for buoys also, in taut mooring it provides the stiffness to the line by providing additional buoyancy while in catenary mooring it supports the anchor by reducing the loads on it through it buoyancy.

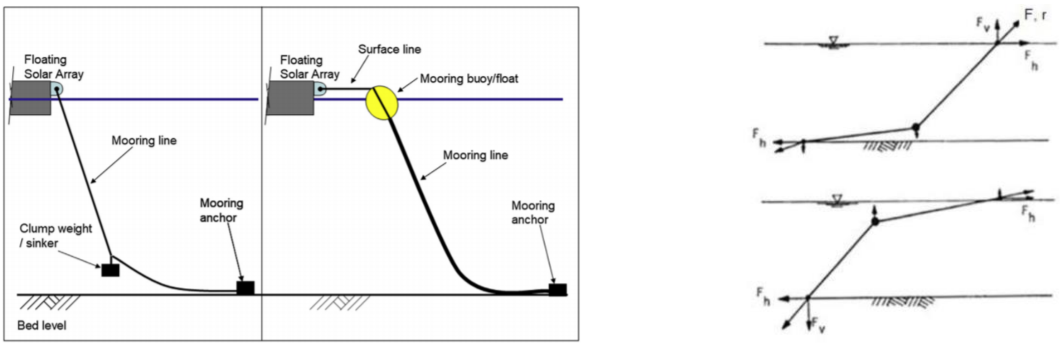


*Figure 2-8: Hybrid Mooring System (Rosa-Clot and Tina, 2020) (Hole, 2018)*

### 2.2.2. Mooring Makeup

Mooring lines can either be made up of single material or can be comprised of a hybrid of materials depending upon the requirement to the particular system. Generally, a hybrid system is used to reduce the weight of the lines in which chains are provided at the top and bottom. In the top, it is provided to increase the tension at the lines due to the self-weight and at the bottom to ensure that there is enough friction resistance and weight required whereas synthetic fibre ropes are provided in the middle to reduce the weight and cost.

#### 2.2.2.1. Chains

Chain is one of the oldest and widely used materials for the mooring lines. There are two kinds of chains used for the same: stud-link chains and studless chains (shown in Figure 2-9) and they come in different grades varying with the properties. Stud-link chains are stronger compared to studless chain, it provides more stability to link and make it easier to handle but are heavier while studless chains are lighter and have better fatigue life, as mentioned in. (Chakrabarti, 2005). Chains have a high abrasion-resistance and heavyweight of it makes it an ideal choice for the catenary mooring. Although care has to be taken while selecting it since it has low fatigue and corrosion resistance. Therefore, it advised to take an oversize chain or use a factor of safety for having a good performance.

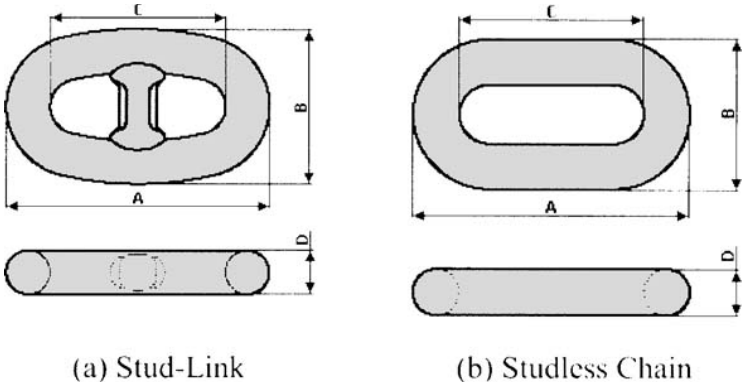


*Figure 2-9: (a) Stud-Link Chain (b) Studless Chain (Chakrabarti, 2005)*

#### 2.2.2.2. *Wire Ropes*

Wires ropes are generally made up of multiple wires of metal (mostly steel) which are twisted together into a helical pattern to form strand which improves the strength and reduces the crushing effect. The wires are denoted by the number of strand and number of wires used in per strand, as shown in Figure 2-10 which are governed by the required strength, fatigue and bending stiffness. Using wire provides better elasticity and lighter weight and low cost compared to the chains for the corresponding strength. Although it has low fatigue resistance and is more prone to damage and corrosion compared to chains, therefore it requires regular inspection and its corrosion life is increased by a coating of the strands or sheathing of the rope.

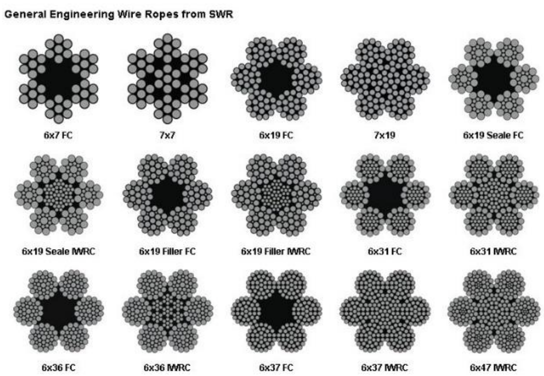


*Figure 2-10: Wire Rope*
[http://web.tradekorea.com/upload_file2/product/292/P00339292/cbe9caa5_111a2f07_f4bb_4f4c_bb6d_d462bc3085d3.jpg](http://web.tradekorea.com/upload_file2/product/292/P00339292/cbe9caa5_111a2f07_f4bb_4f4c_bb6d_d462bc3085d3.jpg)

#### 2.2.2.3. *Synthetic Fibre Ropes*

Synthetic fibre ropes are the most recent material that has been introduced for the mooring lines, shown in Figure 2-11. Being very light in weight, elastic and low in cost compared to chains and wire ropes, it provides a big advantage of using it in deep water as it reduces a large amount of vertical loads as well as it also reduces the complexity in the installation. Additionally, it provides a reduction in extreme and snap loads in the mooring system. Care is to be taken while using it as they are prone to damage from the friction with the seabed, thus the lines are designed in a way to avoid the contact of synthetic fibre rope with the seabed. Another factor that has to be taken care of is the creep and for that regular check-up and tensioning of lines has to be done if the creep is observed of a significant amount.

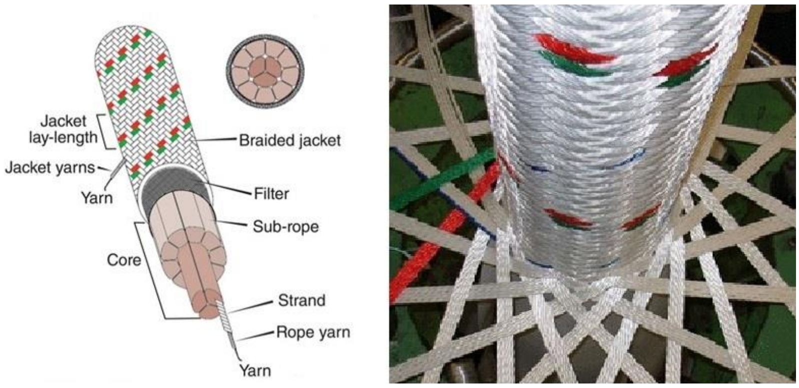


*Figure 2-11: Synthetic Fibre Ropes*
https://sites.google.com/site/deepseamooringsystem/_/rsrc/1375614537375/upcoming-seminars/synthetic/synthetic%20rope%20combined%20picture.jpg?height=189&width=400

## 2.3. Anchoring

Anchors are used for holding the mooring lines in their position. Generally, there is no requirement for a special kind of anchors for the FSPV plant, the anchors used for the other system will be ideal to use in this case too. There is a wide range of anchors, but they can be broadly split into four main categories: deadweight, drag embedment, plate anchors and pile anchors. Selection of the type of anchors for the mooring system depends on different criteria like mooring layout, holding capacity, soil and seabed condition, water depth, the directionality of holding capacity, cost of anchor and installation as well as the installation procedure.

### *2.3.1. Deadweight*

Deadweight is a heavy object usually made by concrete or steel that is placed over the soil. It has a capacity to withstand horizontal and vertical forces because of the self-weight and friction with the soil. Their design can be simple or complex depends upon the requirement of size and weight as well as the holding capacity. Most common designs of deadweight's are sinker, squat clump, mushroom, wedge.

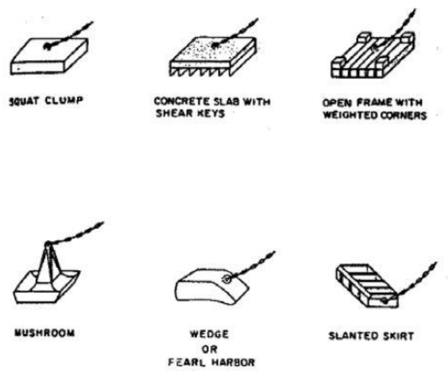


*Figure 2-12: Deadweight Anchors*
https://1.bp.blogspot.com/-yAXmjmwWv80/XnqleQ0jSlI/AAAAAAAAAqI/FAQW2GzaAesyTqUqbrMB7_aEERxbCkMXACLcBGAsYHQ/s1600/13.JPG

These anchors have some pros and cons which has to be taken into account while choosing the anchors which are as followed:

| Pros | Cons |
|---|---|
| • Simple to install as it does not require setting distance.<br>• Reliable anchor because the holding capacity depends on mass. | • Not very efficient anchor (ratio between holding capacity and weight). However, it can be improved with the use of complex shape but it will increase the design cost.<br>• Not suitable when there are big slopes.<br>• Low resistance to lateral loads compared to other anchors; |

Although these anchors are not recommended for offshore applications and big loads since the size of an anchor to withstand the loads you have will be huge and it is not practical neither from the manufacture's point of view nor for installation.

### *2.3.2. Drag Anchors*

These anchors 'dragged' into the seafloor until the fluke penetrates the sea bed. The penetration of the anchor depends on the mooring load, the weight of the anchor and the properties of the soil. The holding capacity is governed by mainly two parameters: fluke area and penetration into the soil. These anchors generally have the hight holding capacity and can sustain load upto 30-40 times of its weight.

*Figure 2-13: (a) Drag Anchor (b) Vertical Load Anchor*
https://img.nauticexpo.com/images_ne/photo-g/68605-11398100.jpg
https://vryhof.com/wp-content/uploads/2020/05/Feature-1_content-768x674.jpg

Although, it has some pros and cons associated with it that has to be taken into account while selecting them and they are as followed:

| Pros | Cons |
|---|---|
| • Relatively simple to install.<br>• The exact position of the anchor depends on the setting distance. | • It does not work well in rocky soils.<br>• It does not work with uplift forces.<br>• Not suitable when there are big slopes.<br>• Requires a mooring line that is parallel to the soil. |

Furthermore, there is a recent development in these kinds of anchors to make them capable of holding vertical loads too and the best example of this development are vertical load anchors. They are installed in a similar way as the drag anchors but penetrated deeper into the soil. And the changing of fluke angle at the desirable penetration enables it to withstand the horizontal as well as vertical loads.

### *2.3.3. Plate Anchors*

As the name justified, these anchors are generally designed in the shape of a plate that is embedded deeply in the soil and is installed in different ways. Holding capacity of these anchors are governed by the surface area bearing against the soil that provides the required resistance. Normally, the plate anchor should be aligned perpendicular to the loading direction to achieve maximum resistance.

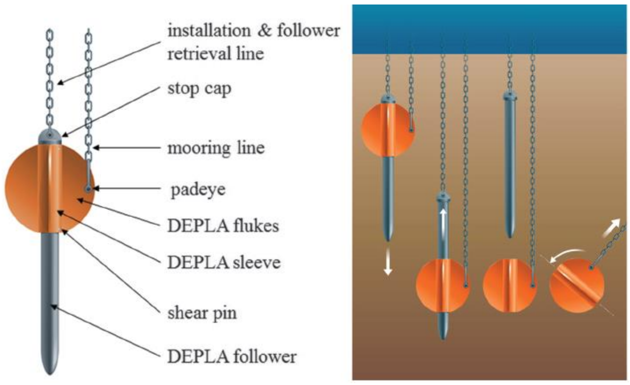

*Figure 2-14: Plate Anchor (Wang and O'Loughlin, 2014)*

The pros and cons related to this anchor are as followed:

| Pros | Cons |
|---|---|
| • Effective in a wide range of soils with different installation techniques.<br>• Higher vertical and horizontal resistance. | • It does not work well in rocky or very soft soils;<br>• Complex to install (depending on the installation technique). Normally three steps: driving the anchor, removing the rods, and load locking.<br>• Anchor cable is susceptible to abrasion. |

### *2.3.4. Pile Anchors*

These anchors are cylindrical, with open-end and made up of steel. They are efficient for almost all soil. They are penetrated in the soil by different installation procedure and the important aspect for these anchors is the point of connection. This point should be deep enough so that it cannot induce the rotation due to mooring loads as generally there is soft clay present on the upper part of sea bed which cannot resist the rotation. They can easily withstand both horizontal and vertical loads.

There are different versions of pile anchors that are mainly differentiated based on the installation process, which are driven pile anchor, suction anchor, torpedo anchor and screw or helicoidal anchors.

*Figure 2-15: (a) Pile Anchor (b) Torpedo Anchor (c) Screw or Helicoidal Anchor*
*https://pbs.twimg.com/media/CcjAFAAUcAAoW7g?format=jpg&name=large*
*https://3kbo302xo3lg2i1rj8450xje-wpengine.netdna-ssl.com/wp-content/uploads/2012/03/DPA-Standing-on-nose-350-x.jpg*
*http://www.alphamarineinstallations.com/graphx/helix_1.jpg*

Pros and cons of these anchors are presented below:

| Pros | Cons |
|---|---|
| • Effective in a wide range of soils with different installation techniques.<br>• Capable of withstanding both horizontal and vertical loads. | • Most complex and expensive in term of installation<br>• Suction piles not suitable for sand, hard clay or granular soil. |

# 3. SITE ASSESSMENT

The starting point for designing the FSPV plant is the site selection which depends on the different aspects like the social aspect, economical aspect, environmental aspect, grid connection. It is designed to install at Hollandse Kust (Noord) wind farm zone (HKN) which is 18.5 kilometres off the west coast of Netherlands. It is intended to place in space between the floating wind turbine (FOWT) to optimise the power production per area. This area is also preferred as it doesn't affect any navigation route of the ship since it is specifically declared for the wind farm. Plus, it can use the existing grid for the power supply. The summary of the individual return period of each environmental condition at the site is presented below which is taken from the report published by (DHI, 2019). Figure 2-1, shows the layout of the HKN wind farm.

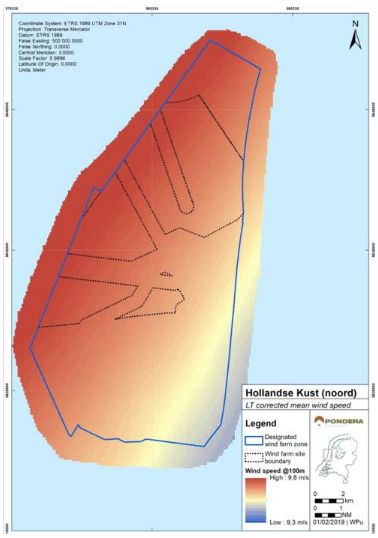


*Figure 3-1: Hollandse Kust (noord)*
*https://ponderaconsult.com/ponderacontent/webinar-wra-hkn-available-online/?lang=en*

## 3.1. Waves

The summary of the wave data proposed for study at the site is presented in the table below. Table 1 provides information about the directional data of significant wave height while Table 2 provides information about the directional peak period of the sea state.

*Table 1: Directional Extreme Significant Wave Heights, High Water (WL > 0mMSL), Hm0 [m]*

| Direction (PWD [deg N]) | Return Period, $T_R$ [years] | | | | | | | |
|---|---|---|---|---|---|---|---|---|
| | **1** | **2** | **5** | **10** | **50** | **100** | **1000** | **10000** |
| **Omni** | **5,56** | **5,93** | **6,39** | **6,71** | **7,33** | **7,60** | **8,38** | **9,03** |
| 0 | 4,34 | 4,79 | 5,30 | 5,68 | 6,44 | 6,68 | 7,51 | 8,23 |
| 30 | 2,15 | 2,58 | 3,01 | 3,30 | 4,05 | 4,42 | 5,30 | 6,18 |
| 60 | 1,18 | 1,47 | 1,72 | 1,94 | 2,31 | 2,46 | 2,89 | 3,24 |
| 90 | 1,12 | 1,37 | 1,59 | 1,79 | 2,18 | 2,31 | 2,70 | 2,99 |
| 120 | 1,00 | 1,25 | 1,51 | 1,78 | 2,19 | 2,33 | 2,73 | 3,06 |
| 150 | 1,23 | 1,45 | 1,74 | 1,96 | 2,40 | 2,51 | 2,96 | 3,31 |
| 180 | 1,85 | 2,11 | 2,41 | 2,60 | 3,13 | 3,51 | 4,53 | 5,30 |
| 210 | 3,37 | 3,73 | 4,21 | 4,54 | 5,15 | 5,42 | 6,09 | 6,72 |
| 240 | 4,74 | 5,04 | 5,41 | 5,68 | 6,23 | 6,51 | 7,22 | 7,90 |
| 270 | 4,57 | 5,01 | 5,53 | 5,87 | 6,56 | 6,82 | 7,60 | 8,22 |
| 300 | 5,08 | 5,51 | 6,00 | 6,32 | 6,97 | 7,21 | 7,99 | 8,63 |
| 330 | 5,17 | 5,62 | 6,14 | 6,50 | 7,20 | 7,47 | 8,27 | 8,96 |

*Table 2: Directional Extreme Associated Significant Wave Periods, High Water (WL > 0mMSL), Tp[s]*

| Direction (PWD [deg N]) | Return Period, $T_R$ [years] | | | | | | | |
|---|---|---|---|---|---|---|---|---|
| | **1** | **2** | **5** | **10** | **50** | **100** | **1000** | **10000** |
| **Omni** | **10,06** | **10,46** | **10,94** | **11,27** | **11,89** | **12,15** | **12,89** | **13,49** |
| 0 | 10,25 | 10,74 | 11,27 | 11,65 | 12,37 | 12,59 | 13,31 | 13,90 |
| 30 | 7,21 | 7,95 | 8,65 | 9,09 | 10,16 | 10,65 | 11,75 | 12,76 |
| 60 | 4,07 | 4,55 | 4,94 | 5,26 | 5,76 | 5,96 | 6,48 | 6,88 |
| 90 | 4,04 | 4,44 | 4,77 | 5,05 | 5,54 | 5,69 | 6,13 | 6,43 |
| 120 | 3,80 | 4,23 | 4,65 | 5,04 | 5,57 | 5,74 | 6,21 | 6,57 |
| 150 | 4,28 | 4,66 | 5,10 | 5,42 | 6,00 | 6,13 | 6,67 | 7,06 |
| 180 | 5,51 | 5,89 | 6,29 | 6,52 | 7,16 | 7,58 | 8,61 | 9,31 |
| 210 | 7,71 | 8,06 | 8,49 | 8,78 | 9,28 | 9,49 | 9,99 | 10,42 |
| 240 | 9,02 | 9,28 | 9,60 | 9,82 | 10,26 | 10,47 | 11,00 | 11,48 |
| 270 | 8,59 | 9,00 | 9,48 | 9,78 | 10,36 | 10,57 | 11,18 | 11,65 |
| 300 | 9,46 | 9,85 | 10,27 | 10,54 | 11,07 | 11,26 | 11,84 | 12,31 |
| 330 | 10,24 | 10,69 | 11,18 | 11,51 | 12,13 | 12,36 | 13,02 | 13,56 |

## 3.2. Winds

The directional wind data for 10-minute average at 10m above the mean sea level is summarized below and tabulated in Table 3.

*Table 3: Directional U10 Wind speeds, 10 m, 10min [m/s]*

| **Directional** | **Return Period, $T_R$ [years]** | | | | | | |
|---|---|---|---|---|---|---|---|
| | **1** | **2** | **5** | **10** | **50** | **100** | **1000** |
| **Omni** | **27,29** | **28,75** | **30,36** | **31,50** | **33,94** | **34,87** | **37,93** |
| 0 | 17,92 | 19,88 | 21,91 | 23,44 | 26,22 | 27,33 | 30,70 |
| 30 | 16,57 | 18,10 | 20,04 | 21,24 | 23,82 | 24,85 | 28,00 |
| 60 | 15,23 | 16,89 | 18,81 | 20,08 | 22,71 | 23,72 | 26,74 |
| 90 | 15,52 | 16,91 | 18,61 | 19,68 | 22,26 | 23,24 | 26,00 |
| 120 | 15,66 | 17,28 | 19,12 | 20,42 | 22,93 | 23,88 | 26,76 |
| 150 | 16,21 | 18,13 | 20,27 | 21,63 | 24,40 | 25,48 | 28,64 |
| 180 | 20,36 | 22,42 | 24,54 | 26,00 | 28,66 | 29,77 | 32,84 |
| 210 | 25,18 | 26,62 | 28,57 | 29,83 | 32,36 | 33,37 | 36,45 |
| 240 | 24,37 | 25,91 | 27,81 | 29,24 | 31,93 | 32,99 | 36,00 |
| 270 | 22,76 | 24,85 | 27,21 | 28,83 | 31,84 | 32,99 | 36,36 |
| 300 | 21,87 | 23,82 | 26,01 | 27,16 | 30,29 | 31,44 | 34,95 |
| 330 | 19,80 | 21,64 | 23,71 | 25,17 | 28,09 | 29,18 | 32,43 |

## 3.3. Currents

For the studies of the mooring system, the current profile will be considered tabulated in Table 5 while the directional current speed at average depth is detailed in Table 4.

*Table 4: Directional total Current speeds – Depth Average [m/s]*

| **Directional** | **Return Period, $T_R$ [years]** | | | | | | |
|---|---|---|---|---|---|---|---|
| | **1** | **2** | **5** | **10** | **50** | **100** | **1000** |
| **Omni** | **1,01** | **1,04** | **1,07** | **1,10** | **1,15** | **1,17** | **1,24** |
| 0 | 1,00 | 1,03 | 1,06 | 1,08 | 1,13 | 1,15 | 1,22 |
| 30 | 1,01 | 1,04 | 1,07 | 1,10 | 1,15 | 1,17 | 1,24 |
| 60 | 0,45 | 0,46 | 0,47 | 0,48 | 0,51 | 0,52 | 0,55 |
| 90 | 0,22 | 0,22 | 0,23 | 0,24 | 0,25 | 0,25 | 0,27 |
| 120 | 0,21 | 0,22 | 0,23 | 0,23 | 0,24 | 0,25 | 0,26 |
| 150 | 0,36 | 0,37 | 0,38 | 0,39 | 0,41 | 0,42 | 0,45 |
| 180 | 0,71 | 0,73 | 0,75 | 0,77 | 0,80 | 0,82 | 0,88 |
| 210 | 0,77 | 0,78 | 0,81 | 0,83 | 0,87 | 0,88 | 0,95 |
| 240 | 0,33 | 0,34 | 0,35 | 0,36 | 0,38 | 0,38 | 0,41 |
| 270 | 0,13 | 0,13 | 0,13 | 0,14 | 0,14 | 0,15 | 0,16 |
| 300 | 0,10 | 0,11 | 0,11 | 0,11 | 0,12 | 0,12 | 0,13 |

| | | | | | | | |
|---|---|---|---|---|---|---|---|
| 330 | 0,15 | 0,15 | 0,16 | 0,16 | 0,17 | 0,17 | 0,19 |

*Table 5: Current Profile [m/s]*

| **Depth (Omni)** | **Return Period, $T_R$ [years]** | | | | | | |
|---|---|---|---|---|---|---|---|
| | **1** | **2** | **5** | **10** | **50** | **100** | **1000** |
| **Near Surface** | 1,50 | 1,54 | 1,59 | 1,63 | 1,70 | 1,73 | 1,83 |
| **75% Water Column** | 1,04 | 1,07 | 1,10 | 1,13 | 1,18 | 1,20 | 1,27 |
| **50% Water Column** | 1,04 | 1,07 | 1,10 | 1,13 | 1,18 | 1,20 | 1,27 |
| **25% Water Column** | 0,97 | 0,99 | 1,02 | 1,05 | 1,10 | 1,11 | 1,18 |
| **5% Water Column** | 0,77 | 0,78 | 0,81 | 0,83 | 0,87 | 0,88 | 0,93 |
| **0% Water Column** | 0 | 0 | 0 | 0 | 0 | 0 | 0 |

## 3.4. Water Levels

The normal water level condition at the site are presented in this section. The site is having a water depth of 24.4m when mean sea level (MSL) is taken as a reference while it is 23.3m when lowest astronomical tide (LAT) taken as the reference. The total variation of water level at the site is the combination of the tide level, non-tidal residual and the mean sea level. The variation of tidal level and the residual level is shown in Table 6.

*Table 6: Water Level Variation*

| **Variable** | **Extreme value - Return Period, $T_R$ [Year]** | | | | | | |
|---|---|---|---|---|---|---|---|
| | **1** | **2** | **5** | **10** | **50** | **100** | **1000** |
| Water level, Total, High [mLAT] | 3,20 | 3,36 | 3,55 | 3,67 | 3,95 | 4,07 | 4,53 |
| Water level, Total, Low [mLAT] | -0,46 | -0,57 | -0,71 | -0,81 | -1,02 | -1,12 | -1,44 |

# 4. DESIGN BASIS

## 4.1. Functional Design Basis

This section gives brief details of the functional requirement of floaters and the mooring that needs to be taken into account while designing them.

### *4.1.1. Floaters*

| Essential | General | Additional |
|---|---|---|
| • Energy Requirement<br>• Articulation<br>• Follow the wave slope | • Space Requirement<br>• Sufficient Air Gap | • Standardization of floater |

#### *4.1.1.1. Essential*

For the reliability of the design, floater had to comply with the essential conditions which are described below:

- The aim is to design the FSPV of 1 MegaWatt (MW) of power which can be used for scaling up power for the project by using multiple plants of 1 MW. This division is done to match the power of inverters and transformers as well as to avoid the crashing of the full plant if a module blacks out, it will only affect that plant and the rest of the plants will still able to run. This principle is currently applied in the onshore plant.
- Articulation should be provided between the floater to ensure that they can easily follow the wave. It will be a flexible joint or a knuckle joint. Their limitation should be studied thoroughly to avoid the collision between the floater as well as provide enough flexibility to follow the wave slope.
- The floater should follow the wave slope to reduce wave slamming as well as to reduce wave forces on the structure.

#### *4.1.1.2. General*

The following requirements are the generic ones that should be followed while designing the floaters for the FSPV plan:

- The utility corridor is provided on the top and bottom of the floater for the cable route and inverter as well as It is also acted for the movement and the maintenance purpose. Similarly, the passage is provided between the modules for the maintenance purpose. The additional spacing is taken between the modules.
- The minimum air gap should be required to avoid slamming from the maximum individual wave height which is expected to break on the floater.

#### *4.1.1.3. Additional*

The additional requirements which can be implied to optimise the design process are as followed:

- The design of the floater should be standardised to optimize the cost required for the production and installation. Although the design will vary with the site as it depends upon the site condition.

### *4.1.2. Mooring System*

This part of the thesis gives the requirement of the mooring system that is considered for the basis of the designing of mooring lines.

| Essential | General | Additional |
|---|---|---|
| • Limiting the excursion of plant<br>• Providing enough flexibility to pant for flowing slope of the wave<br>• Avoid resonance<br>• Reducing the mooring footprint | • Keep loads within the safety factor<br>• Optimize mooring slackness<br>• Avoid out of plane loads<br>• Avoid clashing of mooring lines and power cables<br>• Allow adjustment of cables and future intervention<br>• Reducing fatigue damage | • Optimize the cost of mooring and mooring equipment<br>• Reduce the cost of installation of anchor and mooring line<br>• Minimize vertical loads on the mooring line |

#### *4.1.2.1. Essential*

Good mooring design for the FSPV should comply with the following conditions:

- The excursion of the plant should be limited in all environment condition even in the case of accidental limit state also. This requirement is necessary to ensure that plant does not enter in the area designated for the maintenance vessel.

- To comply with a basic principle of the floater design, mooring lines provided for the plant should be flexible enough to allow the floater to follow the slope of the wave and still maintains the limited excursion of the plant.
- Design of the mooring system should be carefully done to avoid having the resonance with the response of the floater (RAO) in all 6 degrees of freedom.

#### *4.1.2.2. General*

The general requirement that mooring should comply with unless or until it is practical and feasible are summarized below:

- The maximum tension/load generated at any length of the mooring line should be below the breaking load of the respective line taking the account of factor of safety in it.
- The slackness of the mooring line should be optimized to avoid the snap loads and compression in the lines as well the vertical loads generating at the anchors.
- Mooring lines should not clash with anything including the power cables going from the plant to the shore.
- The design of the mooring line should be done in a way to allow the future adjustment in the cables for elongation, creep, settlement.
- Mooring system should have adequate life that exceeds the field life including the fatigue safety factor since it is one of the prominent failure modes.

#### *4.1.2.3. Additional*

Additional requirement for the mooring system which can be implied to optimize the mooring system are summarized below:

- Design of the mooring system should be optimized to reduce the cost of the system (including the lines, anchors and other equipment) and making it more effective.
- The planning of mooring lines should be done in the way to reduce the impact and hazard of the lines on the marine ecosystem as well as a reduction in the installation of the mooring lines.

## 4.2. Environment Design Cases

The analysis for the mooring system is done for the designed criteria formulated based on three limit states ULS, ALS, FLS, as proposed in the (DNVGL-OS-E301, 2018) and their definitions are defined below:

- Ultimate Limit State (ULS): It ensures the individual mooring lines have adequate strength to withstand the load effects imposed by extreme environmental actions.
- Accidental Limit State (ALS): It ensures that the mooring system has adequate capacity to withstand the failure of one mooring line.
- Fatigue Limit State (FLS): It ensures that the individual mooring lines have adequate capacity to withstand cyclic loads.

Since there are no specific rules regarding the design of the FSPV, the mooring design can follow the same rules as of offshore oil and gas facilities with the lower return period for the environmental condition, i.e. 50 years. This return period is also used for designing the moorings of the floating wind turbine (FOWT) which is taken referenced by the different classification society. The lower return period can be justified by two main reasons. First, FSPV is an unmanned facility and only approached for the maintenance purpose which is not likely the scenario with the offshore platform which are usually manned. Second, consequences to the environment due to FSPV mooring failure is lower compared to the similar incident for the offshore platforms/floaters since the risk to the environment is less as they do not handle any hydrocarbons or hazardous chemicals. However, it requires a regular inspection for defects and maintenance purpose.

The information regarding characteristic combined load effect is not available, so it can be obtained by combining individual characteristic load effects due to the respective environmental load types. The combination of those loads are tabulated in Table 7, these combinations are taken from (DNV-OS-J101, 2014). The combinations considered here are to ensure that the combined load effect is with the 50 years of the return period.

*Table 7: Load Combination*

| Load Combination | Wind | Waves | Current | Water Level |
|---|---|---|---|---|
| 1 | 50 years | 5 years | 5 years | 50 years |
| 2 | 5 years | 50 years | 5 years | 50 years |
| 3 | 5 years | 5 years | 50 years | 50 years |

For the analysis, directions of the environmental loads are taken as colinear to obtain the extreme response of the floater for that load combination and seabed is considered to be flat. Table 8 shows different load cases for which the analysis is performed for different limit states. The return period data are taken from the site condition mentioned above and regarding water level, the high water level is considered as it will provide a more severe case compared to low water level since it requires more length of the catenary line. First, the analysis for ULS is done for all their load combination and then analysis for ALS is done for the worst-case among three design cases.

*Table 8: Design Cases*

| Load Combination | Wind | Waves | Current | Water Level |
|---|---|---|---|---|
| 1 | 33,94m/s | 6.39m @ 10.94sec | 1.59m/s @ surface | 27.5m |
| 2 | 30,36m/s | 7.33m @ 11.89sec | 1.59m/s @ surface | 27.5m |
| 3 | 30,36m/s | 6.39m @ 10.94sec | 1.70 m/s @ surface | 27.5m |

## 4.3. Geotechnical Design Basis

The soil information of the seabed is considered uniform with the depth and used for the analysis of mooring system instead of layered soil which makes the analysis more complex. As per data published in (Fugro Survey B.V., 2018), the maximum area of the site is constituted of fine to coarse sand with clay and slit laminae. This property can be outlined with the classification given in (DNVGL-ST-0119, 2018) and its property as per it is defined in Table 9.

*Table 9: Soil Properties*

| Soil type | Friction angle, φ (degrees) | Submerged Unit Weight, γ (kN/m3) |
|---|---|---|
| SAND: Loose to Medium | 28 – 36 | 8.5 - 12.5 |

# 5. DESIGN PHILOSOPHY

## 5.1. Procedure

For the thesis, Ansys Aqwa is used for calculating radiation-diffraction loading that is given as an input to the OrcaFlex in terms of RAO's and QTF's for performing the mooring analysis of the FSPV plant. OrcaFlex is chosen for the dynamic mooring analysis since it is more user friendly and provide more flexibility in modelling articulations which is required for the proposed design. The description of the software and the related theory implemented in this study is provided below which is based on (Ansys, 2017) and (Orcina, 2020).

### *5.1.1. Ansys Aqwa*

Ansys Aqwa software is developed by Ansys, is an engineering analysis suite of tools for the investigation of the effects of wave, wind and current on different types of marine structures. It provides three packages for different analysis requirements: Ansys Aqwa Diffraction, Ansys Aqwa Suite, Ansys Aqwa Suite with Coupled Cable Dynamics. For the thesis, only Ansys Aqwa Diffraction suite is used for obtaining the hydrodynamic data and the related theory has been explained here. This Suite solves the hydrostatic as well as the diffraction-radiation analysis.

Hydrostatics analysis is solved on the panels that describe the submerged part of the body. It uses the same concept of the ship for calculating the stability of the submerged body. Like for checking the stability for the small angle, a body is said to be stable if it's $GM>0$, it will be neutral if $GM=0$ and it has negative stability if $GM<0$. Details of the calculation are given the user manual of Aqwa.

Aqwa uses 3D panel method for analysing the hydrodynamic behaviour of the large-volume structures in wave which is based on the potential flow theory for solving wave inertia load and wave exciting loads and representing the structure by diffracting panels. Both 1st and 2nd order wave loads are calculated. 1st order wave loads are calculated using source distribution method and are represented by the response amplitude operators (RAOs) and the 2nd order wave force are evaluated by the far or near field solution and represented by quadratic transfer functions (QTFs). While Morison approach is used for the slender body and it also provides the possibility of implementing both models when the structure comprises of both large-volume and small cross-sectional components. It can also do the wave diffraction and radiation analysis for the multi-body.

Aqwa solves the set of linear algebraic equations to obtain response amplitude operator (RAO) of the body to regular wave. Eq. (1) defines the set of linear motion equation of M hydrodynamic interaction structures with the frequency-dependent coefficient.

$$\left[-\omega_e^2(M_s + M_a) - i\omega_e C + K_{hys}\right]\left[X_{jm}\right] = \left[F_{jm}\right] \tag{1}$$

Where $M_s$ is a $6M \times 6M$ structural mass matrix, $M_a = [A_{jm,kn}]$ and $C = [B_{jm,kn}]$ are the $6M \times 6M$ hydrodynamic added mass and damping matrices including hydrodynamic interaction coupling terms between different structures, $K_{hys}$ is the assembled hydrostatic stiffness matrix, of which each diagonal 6×6 hydrostatic stiffness sub-matrix corresponding to individual structure and all off-diagonal 6×6 sub-matrices are null as there is no hydrostatic interaction between different structures.

For the slender elements having a diameter of the cylinder, less than 1/5$^{th}$ of the wavelength, defined in (DNV-RP-C205, 2010), the loads on the column are calculated using Morison's approach. This theory assumes that the submerged marine structures have no significant effect on the wave motion as long as the cylindrical diameter is relatively small compared to the wavelength. It is a strip theory which calculates the wave-induced force per unit length which offshore structures are subjected to the inertia term (depending on wave acceleration) and the drag term (depending on square velocity) and integrates it over the length of the structure. Morison's equation for the floating structure given in (3), as proposed by (Chakrabarti, 2005):

$$f = m\dot{u} + f_I + f_D = m\dot{u} + C_M \rho \vec{V} \dot{u} + \frac{1}{2} C_D \rho A |u| u \tag{2}$$

$$f = m\dot{u} + \rho C_M \frac{\pi D^2}{4} \dot{u} + \frac{1}{2} \rho C_D |u| u \tag{3}$$

Where, $f$ is the horizontal wave force acting on the height of the cylinder, $f_D$ is the horizontal drag force, $f_I$ is the horizontal inertial force, $\dot{m}u$ defines the cylinder inertia and $m$ is the mass of cylinder per unit length, $C_D$ is the drag coefficient, $V$ is the volume displacement of unit height, $A$ is the projected area of unit height vertical to the wave motion direction, $u$ is the velocity in the horizontal direction of wave-particle, $C_M$ is the mass coefficient and $D$ is the diameter of the cylinder. The cylinder shape is chosen for the floater as it has the least drag coefficient comparing to other shapes, which helps in minimizing the force acting on the structure.

### *5.1.2. OrcaFlex*

OrcaFlex is a marine dynamic software package developed by Orcina Ltd. The software is capable of performing both static and dynamic analysis in time as well as frequency domain of wide range of offshore systems including mooring. It has an extensive graphical interface in 3D and uses graphs for better understanding of the problem.

It is capable of modelling the motion of the slender elements and uses Morison approach for calculating the wave loads acting on it. Whereas for the motion of larger structures, its hydrodynamic data has to be provided as an input in terms of RAO’s, QTF’s, added mass, damping, stiffness, mass and inertia from the radiation-diffraction analysis based software. It is compatible with importing data from the software like OrcaWave, Ansys Aqwa, WAMIT, MOSES, Hydrostar, WADAM. Based on the input of RAO’s and QTF’s it can calculate both $1^{st}$ and $2^{nd}$ order of wave forces respectively. While it includes current and wind loads through the analytical based method proposed in the design standard.

It provides flexibility in implementing wave, wind and current. It gives the possibility of simulating regular and irregular wave. Regular waves can be model by the following choices: linear wave (Airy Wave) or non-linear waves using Dean, strokes up to $5^{th}$ order or Cnoidal wave. Irregular sea is modelled by the superposition of regular waves and can be defined by the spectrums like JONSWAP, ISSC (Pierson-Moscowitz), Ochi-Hubble, Toresethaugen and Gaussian Spectra.

Furthermore, the wind profile can be defined as the constant or varying with the height above the sea surface. It can also be defined by the spectrums like API and NPD. Current can also be modelled as a constant or with the vertical profile. OrcaFlex provides an option to model these environmental conditions varying with time as well as it also gives an option where a user-defined data can be implemented.

#### 5.1.2.1. *Line Theory*

OrcaFlex uses a finite element model for modelling the mooring lines, shown in Figure 5-1. It divides the line into series of segments that are modelled by massless modal segment connected the node at each end.

Nodes define the mass, weight, buoyancy and drag properties of the line segment. It defines the properties of the half-segment of the line next to it. Forces and moments are applied to the nodes. Whereas the line segment defines the axial and torsional properties of the line. These can be imagined to be made up of two co-axial telescoping rod connect by the axial and torsional spring-dampers. While bending properties are represented by the rotational spring-dampers at each end of the segment, shown in Figure 5-1 (b).

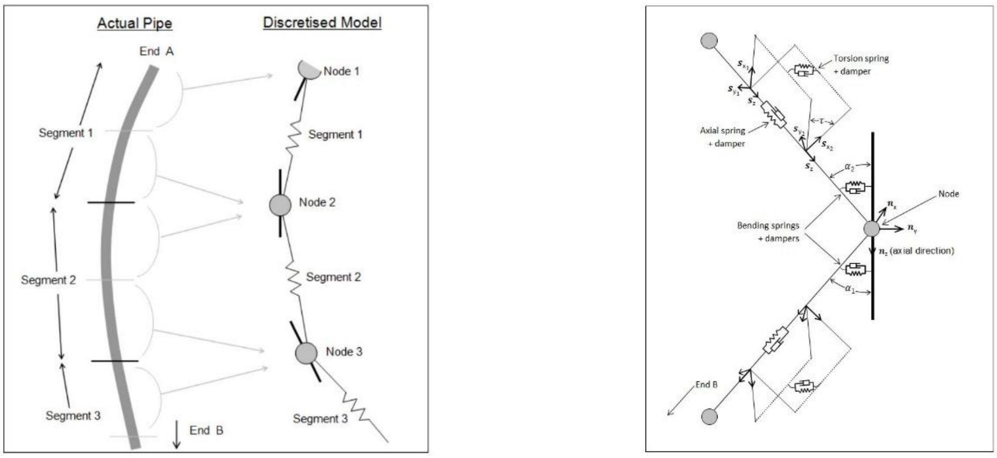


*Figure 5-1: (a) OrcaFlex Line model (b) Detailed Line Model*

#### 5.1.2.2. *Static Analysis*

The main aim of the static analysis is to find the equilibrium configuration of the system under loads applied on it which will also be the starting point of the dynamic analysis. For the linear system, it calculates it with single matrix solver while for non-linear systems it calculates through the iterative approach using a multidimensional form of Newton’s method. The iterative stages in which OrcaFlex determines the static equilibrium are given below:

- In the first stage, it fixes the DOF’s of all the objects (vessels, buoys, constraints, etc) other than the line.

- Then it calculates the equilibrium position for all the lines by solving lines statics.
- In the last stage, it releases all the fix DOF's for determining the equilibrium position of the entire system by performing whole system statics analysis using Newton's Method, taking an initial position for the iteration coming from the above two steps.

#### *5.1.2.3. Dynamic Analysis*

The main aim of the dynamic analysis is to obtain the behaviour and response of the system when it exposed to time-varying loads. It takes the starting point from static analysis which is constant with time. OrcaFlex provides two option for solving dynamic analysis: time domain and frequency domain.

***Time Domain***

Time-domain analysis solves the dynamic analysis problem in the time domain and is a fully non-linear analysis. In this mass, damping, stiffness, loading, etc are calculated at each time step, taking into account of instantons, time-varying values and geometry. OrcaFlex solves the following equation of motion in the time domain.

$$M(p,a) + C(p,v) + K(p) = F(p,v,t) \tag{4}$$

Where,

$M(p,a)$ is the system inertia load

$C(p,v)$ is the system damping load

$K(p)$ is the system stiffness load

$F(p,v,t)$ is the external load

$p, v, a \ and \ t$ are the positions, velocity, acceleration vectors and simulation time

It implements two integration schemes for solving time-domain analysis: explicit and implicit. Both of these schemes solve the motion of equation, Eq. (4 so that it can take account of full nonlinearities. It uses semi-implicit Euler integration with a constant time step for the explicit scheme while generalised-α integration for the implicit scheme. In both schemes, the initial configuration of all nodes is taken from the static analysis and the forces and moment are calculated. Now in the explicit scheme, the local equation of motion is solved for the acceleration vector at beginning of each time step, for each free body and line node, and then integrated using semi-implicit Euler integration. While in the implicit scheme, the system equation is solved at the end of each time step.

***Frequency Domain***

Frequency Domain analysis solves the dynamic analysis problem in the frequency domain and it is a linear analysis. In this analysis, non-linearities are linearized by the process of linearization and it is suited for the stochastic loading. The frequency-domain solver solves the dynamic problem either at wave frequency or low frequency.

The response at the wave frequency is obtained when the system is subjected to first-order dynamic loading associated with the wave elevation stochastic while response at low frequency is obtained when the system is subjected to both second-order waves drift dynamic loading, associated with the wave elevation stochastic process, and wind dynamic loading, associated with the wind velocity stochastic process.

## 5.2. Safety Factors

The factor of safety depends on many factors like analysis type for determining peak loads, redundancy of the system, limit state (intact or damaged mooring system), type of component and classification society. But there is no defined or specific rules or standards for the FSPV by any classification society till now. Therefore, the rules for the floating wind turbines (FOWT) are considered here for the safety factors of mooring lines. The justification for selecting FOWT rules over offshore oil platforms rules for the safety factor will be same as mentioned in the above section mentioning about the selection of the return period of the environmental condition. The safety factor of the mooring line is defined by Eq. (5.

$$SF = \frac{BL}{T_{max}} \tag{5}$$

Where,

$BL$ = Catalogue minimum breaking load of the mooring line component

$T_{max}$ = Maximum Tension occurring over the mooring component during full dynamic mooring analysis

For the thesis, the mooring analysis is done on OrcaFlex using full dynamic analysis. Thus, the factor of safety for the different limit state is taken from (ABS FOWTI, 2013) for the steel mooring lines and summarized in Table 10: Safety Factor for Steel Mooring Lines considering for our working condition.

*Table 10: Safety Factor for Steel Mooring Lines*

| Limit State | Redundancy | Design condition | Safety Factor |
|---|---|---|---|
| ULS | Redundant | Intact | 1.67 |
| ULS | Non-Redundant | Intact | 2 |
| ALS | Redundant | Damaged condition with one broken line | 1.25 |

While for the Fatigue analysis, the calculated fatigue life of the mooring lines should not be less than the design life of the FSPV plant times the fatigue design factor defined in Table 11, which is also taken from (ABS FOWTI, 2013).

*Table 11: Fatigue Design Factor for Fatigue Life of Steel Mooring*

| Redundancy | Inspectable and Repairable | Fatigue Design factor |
|---|---|---|
| Redundant | Yes | 2 |
| | No | 5 |
| Non-Redundant | Yes | 3 |
| | No | 10 |

Based on the safety factor given in Table 10, the limit of allowable breaking load is calculated for the mooring chains used in the thesis for the FSPV plant and it is tabulated in Table 12.

*Table 12: Details of factor of safety and Allowable Breaking Loads for mooring chain*

| **Limit State** | **Mooring Layout** | **Grade** | **Diameter (m)** | **Minimum Breaking Load (tonnes)** | **Factor of Safety** | **Allowable Breaking Load (kN)** |
|---|---|---|---|---|---|---|
| **ULS** | Catenary | R4 | 0.54 | 293.68 | 1,67 | 1725.15 |
| | Hybrid | R3 | 0.60 | 320.8 | 1,67 | 1884.46 |
| **ALS** | Catenary | R4 | 0.54 | 293.68 | 1,25 | 2304.80 |
| | Hybrid | R3 | 0.60 | 320.8 | 1,25 | 2517.64 |

# 6. CONCEPTUAL DESIGN

## 6.1. Floater

The basic idea for the floater is inspired by the movement of attenuator type wave energy convertor on waves as it follows the wave to harness the energy from it. Similarly, an array of floaters is designed to follow the waves. Whereas the designing of a floater is itself a compromise or an optimization between the number of modules and the dimension of the floater. It is intended to maximize the number of modules on it keeping the dimension of floater small enough to follow most of the wave. Maximizing of modules on floater will allow in the reduction of the number of floater and articulation used for joining them. Whereas keeping the dimension of the floater small enough to follow the waves results in the reduction of the air gap and hence increases the stability of the system.

The number of modules used in the project is based on previous experiences of the company and it is scaled down to 1MW. A conservative number of modules is used here (1.2MW) to allow the modification in the top of the floater for additional spaces like vertical access between the floaters and other essential things. These are further divided into smaller groups of modules placed on the floaters. A plant of 1MW consists of 16 floaters, due to confidentiality the sketch of the plant is not shown in this report.

The design proposed here is site-dependent design, more specifically its dimensions depend on the environmental condition at the site. The dimensions of the floater are selected in a way that it can travel over the slope of the wave instead of slamming on it. For acquiring it, the dimensions of the floaters are taken such that it is less than half of the wavelength. Here, the wavelength of the directional waves is calculated using the dispersion relation given in eq. 6, considering the linear wave theory with height equal to significant height and time equal to peak period. Details of directional waves are presented in Table 13.

$$\omega^2 = gk\ \tanh kd \tag{6}$$

$$k = {}^{2\pi}/_{\lambda} \tag{7}$$

Where $\omega$ is the angular frequency, $k$ is the wavenumber, $d$ is the water depth and $\lambda$ is the wavelength.

*Table 13: Directional Wave Details*

| Direction | Significant Wave Height, $H_S$ (m) | Peak Period, $T_P$ (s) | WaveLength, λ (m) | λ/2 |
|---|---|---|---|---|
| 0 | 6,4 | 12,4 | 239,87 | 86.46 |
| 30 | 4,1 | 10,2 | 162,30 | 67 |
| 60 | 2,3 | 5,8 | 52,48 | 26.13 |
| 90 | 2,2 | 5,5 | 47,19 | 23.55 |
| 120 | 2,2 | 5,6 | 48,92 | 24.4 |
| 150 | 2,4 | 6 | 56,16 | 27.9 |
| 180 | 3,1 | 7,2 | 80,87 | 39.05 |
| 210 | 5,1 | 9,3 | 134,92 | 58.79 |
| 240 | 6,2 | 10,3 | 165,50 | 67.91 |
| 270 | 6,6 | 10,4 | 168,73 | 68.81 |
| 300 | 7 | 11,1 | 192,21 | 75.06 |
| 330 | 7,2 | 12,1 | 228,40 | 83.85 |

The floater is designed to align either in north-south direction or east-west direction and only the designed sea state of $H_s$=2.2m (λ=47.19m), coming from 90 degrees and below it will slam on the panel. Accordingly, the air gap of 3.5m is designed considering the maximum individual wave height in that sea state, which is 4m to avoid the slamming on the floating structure. It is designed based on (ABS FOWTI, 2013) standard, which states that a minimum air gap of 1.5 m is to be provided between the 50-year return maximum wave crest elevation above the highest still water level and the lowest edge of the floating support structure. Since it is a conceptual design, a conservative value of air gap is considered which does not take into account the relative motion of floating structure that will result in the reduction of the air gap. For the later design stage, this deck clearance has to be re-examined and optimized with more rigorous theory or by model testing.

Figure 6-1, shows the minimum air gap required to avoid slamming from the maximum individual wave height from the sea state of all direction, tabulated in Table 14 if considering all of them are breaking on the floaters.

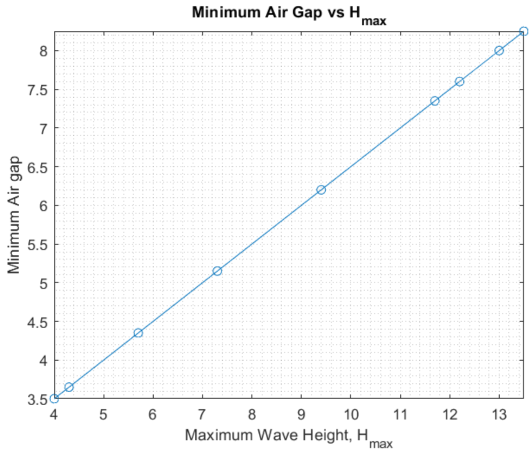


*Figure 6-1: Minimum air gap for different $H_{max}$*

*Table 14: Directional Maximum Individual Wave Height*

| Direction | Maximum Individual Wave Height, $H_{max}$ (m) |
|---|---|
| 0 | 11,7 |
| 30 | 7,3 |
| 60 | 4,3 |
| 90 | 4,0 |
| 120 | 4,0 |
| 150 | 4,3 |
| 180 | 5,7 |
| 210 | 9,4 |
| 240 | 11,7 |
| 270 | 12,2 |
| 300 | 13,0 |
| 330 | 13,5 |

The design of the floater is confidential and therefore does not presented in this report. The floater is made up of mild steel (density = 7800mg/m³). The Static stability of the floater for small heel and trim angle is checked using Eq. (8) and Eq. (9) and ensured that both the transverse and longitudinal metacentric heights are greater than zero.

$$GM_T = KM_T - KG = KB + BM_T - KG \tag{8}$$

$$GM_L = KM_L - KG = KB + BM_L - KG \tag{9}$$

$$BM_T = \frac{I_T}{\nabla} \tag{10}$$

$$BM_L = \frac{I_L}{\nabla} \tag{11}$$

Where, $GM_T$ is transverse metacentric height, $GM_L$ is longitudinal metacentric height, $KG$ is the vertical centre of gravity, $KB$ is centre of buoyancy, $I_T$ is the transverse second moment of the water-plane area about the centreline, $I_L$ is the longitudinal second moment of the water-plane about the centre of flotation, $\nabla$ is volume displaced by the floater.

The beams are made up of steel as well and it is selected based on bending analysis taking into account of the self-weight of the plant, further FEM analysis is required for verifying the scantling for the hogging and sagging loads.

Articulations are used to connect the unit floaters and make them able to follow the slope of the wave easily. But unfortunately, at this stage, there is no knowledge about the design of the articulation due to the lack of data of the forces as well as the expertise about the articulation. It is just considered flexible enough to flow the slope of the wave. For designing of the articulation, maximum individual wave height should consider that the floater is expected to follow is considered and the analysis is done based on it as it will be the most critical scenario. It has to be ensured in this scenario that the angle made by the articulation should be restricted when the articulation centre is just above the crest to avoid collision and to have a minimum horizontal distance between the lower tip of the floater.

### *6.1.1. Analysis of Single Floater*

This section gives the details about the initial analysis done on the floater for hydrostatic and estimation of viscous damping.

#### *6.1.1.1. Mass Properties*

Table 15 gives the details of the mass properties of a single floater that has been inputted to Aqwa to study the hydrostatic analysis and dynamic diffraction of a single floater and later on provided to each floater in the plant.

*Table 15: Mass Properties of Floater*

| | | |
|---|---|---|
| Mass | 25.533 | tonnes |
| Centre of Gravity X | 12.16 | m |
| Centre of Gravity Y | 11.85 | m |
| Centre of Gravity Z | 2.792 | m |
| Radius of Gyration, Kxx | 7.793 | m |
| Radius of Gyration, Kyy | 7.183 | m |
| Radius of Gyration, Kzz | 10.291 | m |

#### 6.1.1.2. *Hydrostatics*

Table 16 shows the results of the hydrostatic analysis done on the Ansys Aqwa. It can be inferred from the result that the floater is stable as it had GM>0.

*Table 16: Hydrostatics*

| | | |
|---|---|---|
| Actual Displacement | 24.91 | $m^3$ |
| Centre of Buoyancy X | 12.16 | m |
| Centre of Buoyancy Y | 11.85 | m |
| Centre of Buoyancy Z | 0.5 | m |
| Metacentric Height, GMx | 49.58 | m |

#### 6.1.1.3. *Damping*

Ansys Aqwa is a potential flow solver, to incorporate the viscous damping effect, additional damping is introduced for roll, pitch and heave. For this study, diffraction-radiation analysis is performed on the single floater and additional linear critical damping is taken for roll, pitch and heave. These values are taken based on the previous experience of the company. Generally, these values are used for the vessels mainly but due to insufficient information for the floaters, these values are taken as the reference for the initial design stage and has to be to verify with model testing.

## 6.2. Mooring System

### 6.2.1. *Diffraction Analysis*

Ansys Aqwa is used for calculating diffraction-radiation loading of the floater. Although the length of the column is small enough to consider them as the Morison element but presence of column in close proximity within the floater as well as with adjacent floater creates the hydrodynamic interaction between the columns. This effect cannot be modelled through the Morison equation so, it required a diffraction-radiation analysis.

The mesh details used for the hydrodynamic diffraction analysis of the full plant cannot be shown in this report due to the confidentiality. The maximum element size is taken as 0.8m, the finer mesh was not possible since Aqwa has the limitation in number of elements of 40,000 and going finer than this element size was resulting in breaking of mesh in the lower part of the floater because of multiple structures. Additional studies were performed to see the sensitivity analysis for the element size considering the single floater and it was found that there was not much difference in the result. Although, it will be more accurate if the finer mesh was possible but it will take more computation time as well as space.

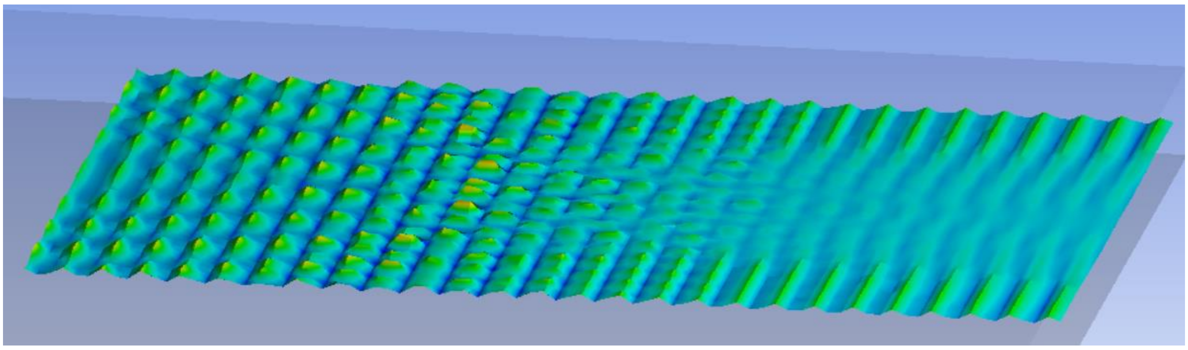

*Figure 6-2: Wave Surface Elevation*

Figure 6-2 shows the wave surface elevation and it can be inferred that the effect of the hydrodynamic interaction between the column in the wave field as the wave surface elevation is dampened which is visible by the progressively decreasing of the wave elevation from the starting to the end.

Figure 6-3 shows the RAO's value in heave and pitch for a row of floaters when the wave is coming from 0 degrees. It can be seen that RAO's are decreasing from the floater that is directly facing the wave (have biggest RAO) to the floater that is farthest (have the lowest RAO). This also explains the hydrodynamic interaction between the column. RAO's of the other degree of freedom are presented in AppendiX A

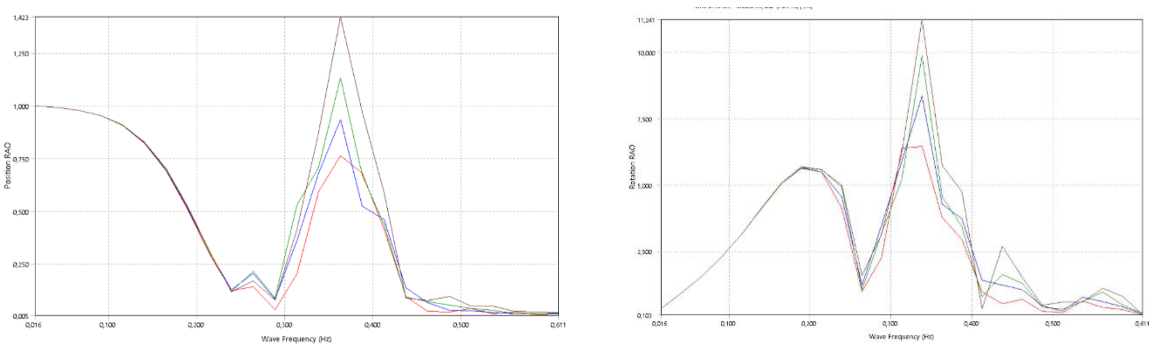


*Figure 6-3: RAO's (a) Heave (b) Pitch*

### 6.2.2. Forces

#### 6.2.2.1. Waves

As mentioned before the method for calculation of wave forces depends upon the dimension of the size of the structure. The wave forces on the large structure are calculated by the diffraction-radiation analysis while the wave forces for the slender element is calculated by the Morison approach.

For the floater, diffraction-radiation analysis is used to model the interaction between the structures. This is performed in Ansys Aqwa software and the output from it as RAO's and QTF's, are inputted in OrcaFlex which calculates the first order and second-order wave forces from it respectively during the dynamic analysis. Irregular wave is considered for the dynamic simulation and it is defined by Jonswap spectrum with gamma taken as 3.3 for the north sea, as suggested in (DNVGL-OS-E301, 2018).

#### 6.2.2.2. Wind

Wind forces are induced due to the wind pressure acting in the direction normal to the surface of the structure that is above the water. These forces can be steady or time-varying depends on the fluctuation in the wind speed. The response to the wind load is superimposed with the static response and the resonant response due to excitation close to the natural frequency. Wind speed is generally measured at the altitude of 10m. The wind force for the initial calculation can be calculated from the analytical method described below by the equation:

$$F_{wind} = \frac{1}{2} C_S \rho_{air} A V_w^2 \tag{12}$$

Where,

$F_{wind}$ = wind force (N)

$\rho_a$ = density of air (kg/m$^3$)

$C_S$ = shape coefficient in a steady flow

A = projected area of structure normal to the direction of force (m$^2$)

$V_w$ = wind velocity at the given elevation (m/s)

For the FSPV, wind forces are important due to a large number of panels on the floaters. Although these forces are minimised by tilting these panels at the small angle of 11 degrees. The value of tiltation angle is selected by the previous experience of the company to capture the maximum amount of sunlight. This value has to be verified in the later studies for the offshore condition since it was based on the studies done for the FSPV plant in onshore condition.

Wind loads acting on a tilted solar panel are influenced by a large number of factors such as wind direction and magnitude, solar panel size and tiltation angle, ground clearance and space between the panels. In this study, the effects of shelter and wind wake are not taken into account and the force on one panel is multiplied with the total number of panels to get the total force on the panels. In order to take into account, the above-mentioned effects, it is recommended to perform CFD analysis and this can lead to a substantial reduction in wind forces.

The shape coefficient depends upon the Reynolds number of the wind flow. Due to the lack of available data for the shape/drag coefficient for the panels in offshore condition, these data have taken from the studies for the ground-based panels done by (Irtaza and Agarwal, 2018) and (Agarwal et al., 2017). From these studies, the drag coefficients for the 11 degrees of tiltation angle has taken for a different angle of attack directions, which is tabulated in Table 17. For the analysis, panels are considered to be oriented at 90 degrees and a support frame for the panel is considered as a cube. The value of the shape coefficient for it and freeboard part are taken from (DNV-RP-C205, 2010). In the analysis, to be in the conservative side, constant wind speed at all height above the sea surface is considered instead of the spectrum. It will be also enthralling to use wind spectrum and that can have an impact in the dynamic motions of the platform.

*Table 17: Drag Coefficient for the Solar Panel*

| Wind Blowing Direction (from) | Drag Coefficient in panels (wind direction) |
|---|---|
| -180 | 0.023 |
| -135 | 0.068 |
| -90 | 0.102 |
| -45 | 0.068 |
| 0 | 0.023 |
| 45 | 0.077 |
| 90 (panel Orientation direction) | 0.116 |
| 135 | 0.077 |

The lift forces on the panels are considered negligible in this stage and assumed that it will be self-balanced by the buoyancy, self-weight and the mooring effect. The accurate estimation of lift forces is extremely challenging as they depend both on the large-scale flows around the body as well as the small-scale flows close to the body surface that dictate whether the flow separates from the body. In the future design stage, it is recommended to refer to physical modelling results to make a reasonable estimate of these forces.

Wind loads are calculated using standard OCMIF method in the OrcaFlex and it requires the coefficient values in all degree of freedom. For this study, only the drag value in surge and sway are considered for the including in low-frequency motion. Therefore, an equivalent coefficient for the structure above sea level is calculated and inserted in the software, shown in Figure 6-4.

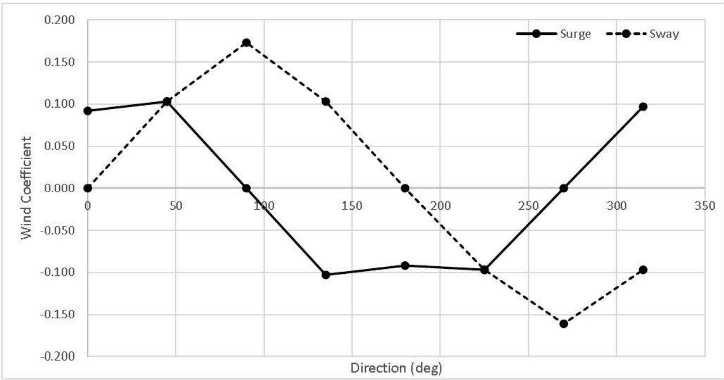


*Figure 6-4: Wind Coefficient (OrcaFlex input)*

#### 6.2.2.3. Currents

Current induced forces act on the all submerge object associated with FSPV like submerge part of the floater, mooring lines, electric cables, etc. For the initial calculation it can be calculated by the analytical method, later on, it has to be verified with the model testing and full-scale measurements. These loads cause large steady and slow drift motion of the moored structure. Therefore, it important to have better results in the initial stage so instead of constant current, its vertical profile at the site has to be used for its velocity.

The current forces are calculated as the drag force acting on the submerged part of the structure and it is given by the following equation:

$$F_{current} = \frac{1}{2} C_d \rho_{sw} A u_c |u_c| \tag{13}$$

Where,

$F_{current}$ = current force (N)

$\rho_{sw}$ = density of sea water (kg/m$^3$)

$C_d$ = drag coefficient in a steady flow

A = projected area exposed to current (m$^2$)

$u_c$ = current velocity normal to the projected area (m/s)

Drag coefficient depends on the smoothness of the surface and the Reynolds number of the flow and it is taken from (DNV-RP-C205, 2010) considering them smooth, having large KC. Current velocity is considered as steady and its profile is taken from (DHI, 2019) and mention in the above section.

Current loads are also calculated using standard OCMIF method in the OrcaFlex and it requires the coefficient values in all degree of freedom. For this study, only the drag value in surge and sway are considered for the including in low-frequency motion. Therefore, an equivalent current coefficient for the structure below sea level is calculated and inserted in the software, given in Figure 6-5. Moreover, CFD can be an added value, since more accurate coefficients can be obtained from it.

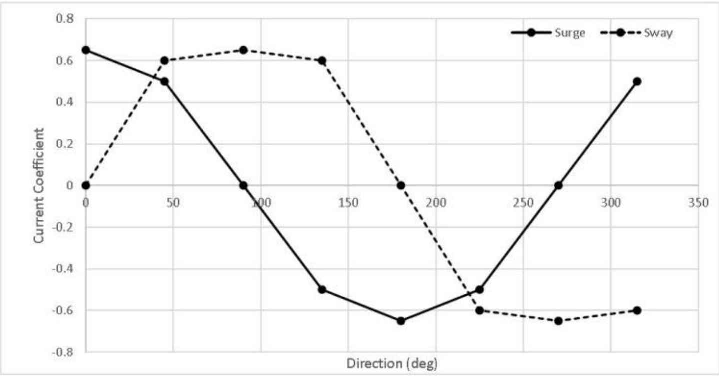


*Figure 6-5: Current Coefficient (OrcaFlex input)*

# 7. MOORING ANALYSIS

## 7.1. Model Setup

The mooring system of the plant is one of the main systems that need to be studied thoroughly as it constitutes the major part of the total cost of the system. Thus, the optimization of this system can save a lot of budgets. The selection of the layout of the mooring system depends on many criteria like type of floater, redundancy, cost of the mooring system and installation, and in this case, it should also base on the criteria that are mentioned in the mooring requirement.

In this study, selected mooring layout of the system is not fully optimised, it is based more on optimizing cost and easiness in the installation of the system although it will have a disadvantage in the terms of mooring footprint as it requires larger area. To overcome that problem only chains are considered for the mooring line. Since it is the initial study based on many assumption and conceptual calculations as well as the time constraint, it is good to start with an approach and having a magnitude of the forces and mooring footprint. Even at this stage export cables are not included which may cause some interference with the mooring system. Later on, after having the studies about the other issues like structural details, especially about the articulations and electrical cabling it will be interesting to study the other optimize mooring layouts as that time the response and movement of the floater will be much closer to the reality. Actually, for this type of systems which has to place in the vicinity of the FOWT, the mooring system should be the optimisation between the overall cost and the mooring footprint of the system.

The attachment of the mooring lines is done in a way that it provides redundancy to the system, sustain in environmental loads from all direction and to avoid the concentration of mooring loads at a single point. Due to confidentiality, the setup of the floaters is not shown in this report. These conditions are considered for the safety of the plant to reduce the chances of collision in case of mooring damage as it will be placed in the proximity of the FOWT and passing by ships. The failure in the mooring system will also imply high reparation costs, not only in the mooring line but also in disconnection with the export cable, the mobilization of an offshore construction vessel and damaging the cables.

The design of the articulation is the biggest challenge for the success of this design of the FSPV and it has to be studied in detail after the structural analysis so that it can be designed to resist the loads acting on it at the same time provides the required flexibility to the system to flow the slope of the wave without colliding with each other. For modelling purposes only one articulation is considered, in practice, it can be many to transfer properly the loads effectively among the floaters that also has to be studied in detailed. At this initial stage, due to the lack of data of the forces and the knowledge about the articulation, an assumption has taken to model these articulations. The articulations which are connecting the floater in the row, there translational degree of freedom (DOF) in heave and rotational DOF along axis $xx'$ are released. While the articulation which are connecting the floaters in the column, there translational DOF in heave and rotational DOF along axis $yy'$ are released. Also, the stiffness and damping at articulation are not considered. This will infact give some extreme values in the motion of floater as well as the tension in the mooring lines at some frequencies which are not even possible in reality. Further, the result of the maximum tension and excursion from the dynamic analysis will be a conservative value. These articulations are modelled as a combination of a constraint and a small massless high stiffness line in OrcaFlex. The floater is connected with the constraint while the line is connected with the constraint to another floater and the flexibility of this joint is controlled by the constraint.

For the analysis, panels are considered to be oriented in 90 degrees and to have the worst effect of the environmental loading (wave, wind and current) on the plant their directions are taken colinear and considered to be coming from 90 degrees.

This section gives details about the different model setup and following it, discussion about the results of the analysis is done. The simulations are run for 3600 seconds or 1 hour of the sea state.

### *7.1.1. Base Case*

The base case or the starting point of designing of mooring system is taken from general mooring layout used for the other system. Later on, the modification is done to optimise this layout as per the requirements mentioned in the above section. Among the general layouts, catenary mooring is selected as a base case since it is easiest and cheapest to install, due to confidentiality the layout of the system is not shown in this report.

For this case, R4 grade chain of 54 mm nominal diameter having a minimum breaking load of 293.68 tonnes is used. The line has a length of 486m anchored at a distance of 480m from the floater. The length of the lines is taken long enough to ensure there is enough laying length in extreme load cases presented in ULS as well as in ALS. For the simulation, the primary motion is treated as the combination of both low and wave frequency, and the dividing period for this case is taken as 13.19 seconds which is based on Eq. (14), taken from (Browne, 2013).

$$T_d = \frac{1}{2(f_{wf} + f_{Lf})} \tag{14}$$

Where, $T_d$ is the dividing period, $f_{wf}$ is the wave frequency which is taken as the peak period of the spectrum and $f_{Lf}$ is the low frequency taken from the highest natural period from the decay test in OrcaFlex.

### *7.1.2. Hybrid Case*

Hybrid case is the optimizes version of the above base case of catenary mooring system which is optimized keeping in mind to minimize the mooring footprint. For the same, sinker or clump weight has been used which provide the support to the anchor by taking part of the load, due to confidentiality the layout of the system is not shown in this report. This makes it possible to reduce the line length and still having enough laying length. This layout is not the most optimised version more optimised version may be possible but it will be more interesting to study it after have more information about the articulation which will provide better knowledge of the movement of the floaters that will be closer to the actual movement.

In this case, R3 grade chain of 60mm nominal diameter having a minimum breaking load of 320.8 tonnes is used. The line has a length of 170m anchored at a distance of 160m from the floater. Dividing period for this case is taken as 16.5 seconds.

## 7.2. Results

This section deals with results of the dynamic mooring analysis which were performed on the layout mentioned above.

### *7.2.1. Base Case*

This section summarised the results of the dynamic mooring analysis performed on the base case for the 3 load cases of ULS and 1 load case of ALS. It is not feasible to show the results of all line. Therefore, the results of the lines that are directly facing environmental load (i.e. line 3 and 4) are presented and it is interesting to see them since they have the highest tension among all lines. The maximum tension in the line will be at fairlead where the top end of line is connecting with the floater. The time series of the effective tension occurred in line 3 and 4 for all load cases of ULS are shown in Figure 7-1, Figure 7-2 and Figure 7-3.

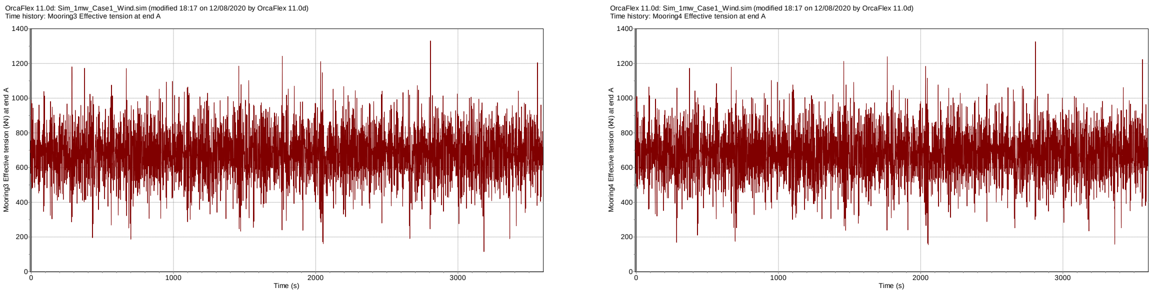


*Figure 7-1: ULS – Load Case 1 – Tension (kN) in (a) Mooring line 3 (b) Mooring Line 4*

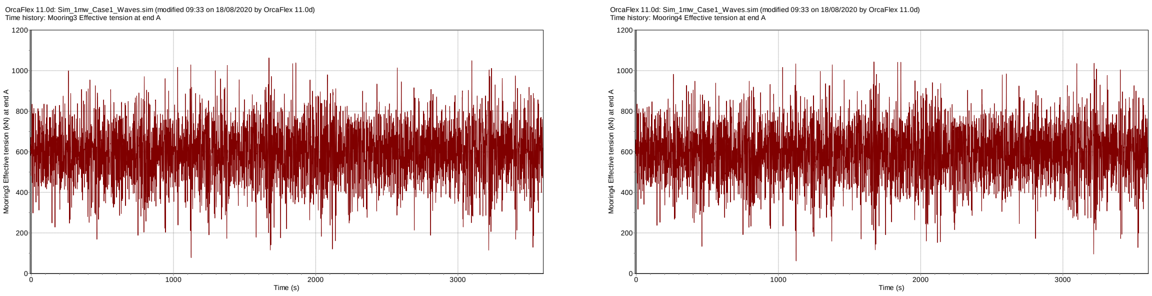


*Figure 7-2: ULS – Load Case 2 – Tension (kN) in (a) Mooring line 3 (b) Mooring Line 4*

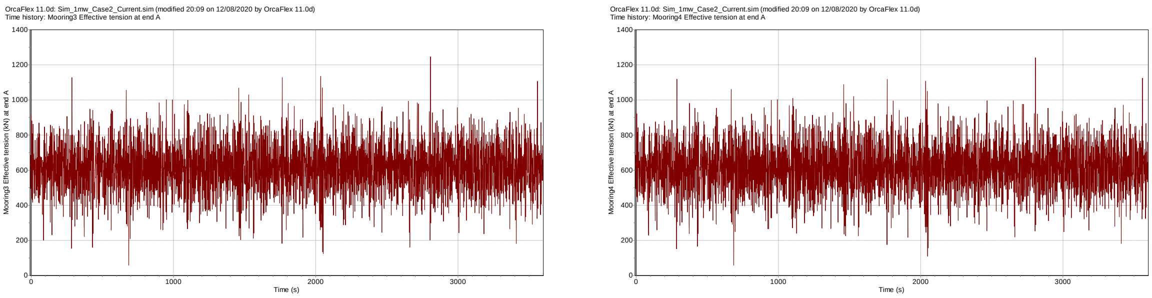


*Figure 7-3: ULS – Load Case 3 – Tension (kN) in (a) Mooring line 3 (b) Mooring Line 4*

It can be noted from the above figures that the tension in line 3 is slightly higher than the line 4 which is mostly due to the yaw moment of the floaters, it was expected since a small magnitude of RAO was observed in the yaw motion from the diffraction-radiation analysis performed in Ansys Aqwa (shown in AppendiX A). The mean tension from the graph shows the contribution of loading from the wind and current to the floater that is maximum for the wind due to the presence panels.

It can also be inferred from the figures that worst case in the ULS is load case 1 since maximum effective tension has occurred in this case in line 3, i.e. 1329.30kN. Thus, for the ALS load case 1 is considered with line 3 as broken and the time series of the effective tension in line 4 is shown in Figure 7-4.

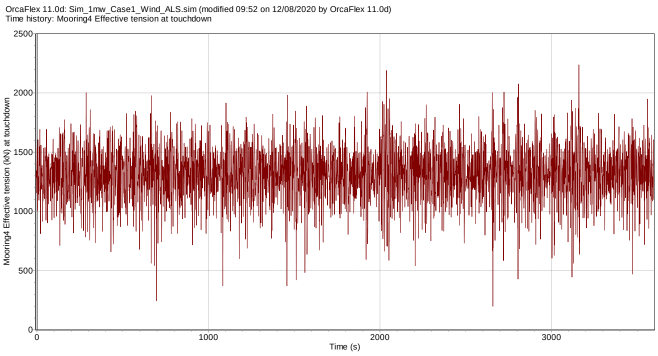


*Figure 7-4: ALS – Load Case 1 – Tension (kN) in Mooring line 4*

The summarised result of the tensions and laying length are tabulated in Table 18 and

Table 19.

*Table 18: Base Case: Summarised Result of Line 3*

| Limit State | Load Cases | Effective Tension at Line 3 (Platform End) | | | | Min Laying Length (m) | Effective Tension in Line 3 (Anchor End) | | | |
|---|---|---|---|---|---|---|---|---|---|---|
| | | Min (KN) | Max (KN) | Mean (KN) | Standard deviation (KN) | | Min (KN) | Max (KN) | Mean (KN) | Standard deviation (KN) |
| ULS | 1 | 115,18 | 1330,74 | 682,60 | 136,56 | 145,00 | 158,20 | 1329,30 | 681,91 | 117,89 |
| | 2 | 78,19 | 1062,99 | 597,61 | 132,24 | 180.00 | 121,19 | 1040,34 | 596,70 | 111,32 |
| | 3 | 58,14 | 1246,90 | 617,66 | 128,75 | 155,00 | 108,67 | 1241,27 | 617,37 | 108,14 |
| ALS | 1 | Broken | | | | | | | | |

*Table 19: Base Case: Summarised Result of Line 4*

| Limit State | Load Cases | Effective Tension at Line 4 (Platform End) | | | | Min Laying Length (m) | Effective Tension in Line 4 (Anchor End) | | | |
|---|---|---|---|---|---|---|---|---|---|---|
| | | Min (KN) | Max (KN) | Mean (KN) | Standard deviation (KN) | | Min (KN) | Max (KN) | Mean (KN) | Standard deviation (KN) |
| ULS | 1 | 155,35 | 1325,94 | 682,98 | 135,70 | 145,00 | 178,33 | 1325,05 | 682,83 | 116,64 |
| | 2 | 61,66 | 1043,47 | 596,51 | 131,45 | 180.00 | 88,98 | 1027,07 | 596,01 | 110,46 |
| | 3 | 58,36 | 1241,33 | 617,80 | 127,77 | 160,00 | 102,87 | 1233,41 | 618,22 | 106,66 |
| ALS | 1 | 306,78 | 2193,77 | 1318,79 | 202,54 | 34,00 | 239,89 | 2221,32 | 1315,64 | 193,35 |

From the above table, it can be inferred that the tension is maximum for the load case 1 for the ULS which has had the largest wind speed. It was already expected since the wind loads on the panels will be dominant in FSPV and it will generate a large force which will be counterbalanced by the mooring lines. Thus, having maximum effective tension for this case is reasonable. Due to the wind dominating factor it can also be seen that the mean tension is also high compared to the other cases. This large peak loads and high standard deviation indicates that the fatigue during the storm will be a significant factor and need to be considered. By comparing the mean tension in load case 2 and 3, it can be said that current loads have more influenced in the drag forces compared to second-order load by waves. This dominating effect comes from the lower circular beam provided to make the floater rigid. It can also be seen from the above table that there is enough laying length even in both limit state as well as maximum tension generated for limit state, i.e. ULS and ALS are under the allowable breaking limit given in Table 12 (ULS-1725.15 kN and ALS-2304.80 kN) that, justifies the reasonability for the choice of the chain size.

It is also not interesting and feasible to see the motions of all floaters. Therefore, the details of floaters at the extreme corners have been reported for the movement of the plant in different degree of freedom. The motions in heave and roll are not reported since those DOF's are free and having some extreme values of some frequency which are not possible in reality. It will be enthralling to observe those results after having a better knowledge of articulation.

Table 20 and Table 21 shows the maximum amplitude from the mean position and the maximum acceleration of the extreme floaters respectively to see the overall motion of the plant. It is interesting to see the amplitude of mean position for both limit state and the acceleration for ULS since ALS will no doubt have the high acceleration as a line is broken. The probability of having a condition of one broken line will be in the storm condition and the acceleration at that time will be not much important as it will be unmanned during that time but the excursion will be important to see since the collision can occur during that time.

*Table 20: Base Case: Maximum Amplitude from Mean Position*

| ULS - Load Case 1 | | | | |
|---|---|---|---|---|
| Floater No. | Maximum Amplitude from Mean Position | | | |
| | Surge (m) | Sway (m) | Pitch (deg) | Yaw (deg) |
| **1** | 0,93 | 6,45 | 4,39 | 1,09 |
| **4** | 1,09 | 6,46 | 4,61 | 0,89 |
| **13** | 1,29 | 6,38 | 5,02 | 0,97 |
| **16** | 1,37 | 6,40 | 4,03 | 1,35 |

| ULS - Load Case 2 | | | | |
|---|---|---|---|---|
| Floater No. | Maximum Amplitude from Mean Position | | | |
| | Surge (m) | Sway (m) | Pitch (deg) | Yaw (deg) |
| **1** | 0,61 | 6,34 | 4,26 | 0,74 |
| **4** | 0,62 | 6,30 | 4,25 | 0,97 |
| **13** | 0,87 | 5,86 | 4,49 | 0,93 |
| **16** | 0,98 | 5,81 | 4,06 | 0,99 |

| ULS - Load Case 3 | | | | |
|---|---|---|---|---|
| Floater No. | Maximum Amplitude from Mean Position | | | |
| | Surge (m) | Sway (m) | Pitch (deg) | Yaw (deg) |
| **1** | 0,59 | 6,16 | 3,98 | 0,96 |
| **4** | 0,70 | 6,16 | 4,78 | 0,86 |
| **13** | 0,79 | 6,06 | 5,03 | 0,95 |
| **16** | 0,75 | 6,11 | 3,82 | 0,89 |

| ALS - Load Case 1 | | | | |
|---|---|---|---|---|
| Floater No. | Maximum Amplitude from Mean Position | | | |
| | Surge (m) | Sway (m) | Pitch (deg) | Yaw (deg) |
| **1** | 5,36 | 17,92 | 5,29 | 8,59 |
| **4** | 5,70 | 7,90 | 9,16 | 7,58 |
| **13** | 5,49 | 16,73 | 9,83 | 7,99 |
| **16** | 4,97 | 7,21 | 5,50 | 8,15 |

The horizontal motions such as surge and sway are much more influenced by the mooring system as it provides the horizontal restraint. The environmental loads are coming from 90 degrees therefore, it can be seen that the dominating motion of the plant is in sway motion and the maximum amplitude from the mean position and acceleration is observed of about 6.4m and 5m/s$^2$ respectively for the load case 1 in the ULS. While in the ALS, the floaters in the side at which the line is broken will have maximum motion, amplitude and acceleration of about 17.9 m. In the ULS case, it can be seen that the motions in the load case 2 is higher than the load case 3, it is due to the dynamic loading of the wave on the floater.

*Table 21: Maximum Acceleration*

| ULS - Load Case 1 | | | | |
|---|---|---|---|---|
| Floa ter No. | Maximum Acceleration | | | |
| | Surge (m/s$^2$) | Sway (m/s$^2$) | Pitch (rad/s$^2$) | Yaw (rad/s2) |
| **1** | 1.96 | 5.52 | 0.95 | 0.25 |
| **4** | 2.10 | 4.61 | 0.60 | 0.25 |
| **13** | 1.42 | 3.74 | 0.48 | 0.25 |
| **16** | 1.53 | 4.09 | 0.52 | 0.25 |

| ULS - Load Case 2 | | | | |
|---|---|---|---|---|
| Floa ter No. | Maximum Acceleration | | | |
| | Surge (m/s$^2$) | Sway (m/s$^2$) | Pitch (rad/s$^2$) | Yaw (rad/s2) |
| **1** | 1.85 | 3.50 | 0.80 | 0.20 |
| **4** | 2.03 | 3.18 | 0.57 | 0.21 |
| **13** | 1.50 | 3.77 | 0.41 | 0.26 |
| **16** | 1.81 | 3.63 | 0.43 | 0.24 |

| ULS - Load Case 3 | | | | |
|---|---|---|---|---|
| **Floater No.** | **Maximum Acceleration** | | | |
| | **Surge ($m/s^2$)** | **Sway ($m/s^2$)** | **Pitch ($rad/s^2$)** | **Yaw (rad/s2)** |
| **1** | 2.01 | 5.25 | 0.90 | 0.20 |
| **4** | 1.89 | 4.45 | 0.66 | 0.21 |
| **13** | 2.41 | 4.36 | 0.57 | 0.21 |
| **16** | 3.18 | 5.59 | 0.49 | 0.27 |

### *7.2.2. Hybrid Case*

This section summarised the results of the dynamic mooring analysis performed on the hybrid case for the load cases in ULS and ALS. Here also it is interesting to see the results for the lines that are directly facing environmental load only since they have the highest tension among all lines (i.e. line 3 and 4). The time series of the effective tension occurred in line 3 and 4 for all load cases are shown in Figure 7-5, Figure 7-6 and Figure 7-7. And the summarised result of the tensions and laying length are tabulated in Table 22 and Table 23.

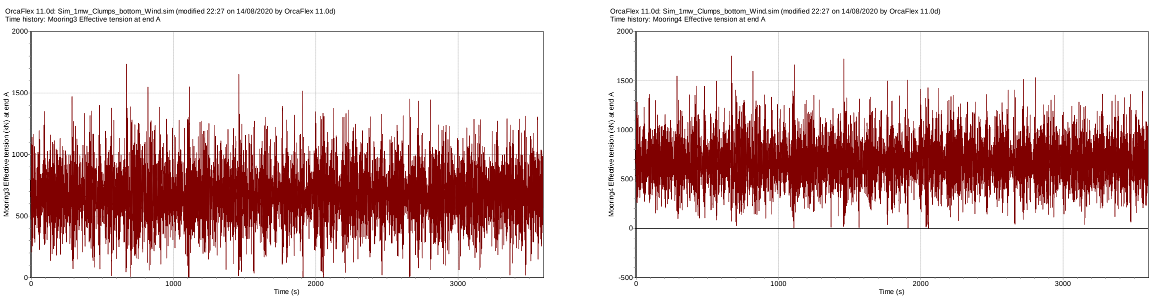


*Figure 7-5: ULS – Load Case 1 – Tension (kN) in (a) Mooring line 3 (b) Mooring Line 4*

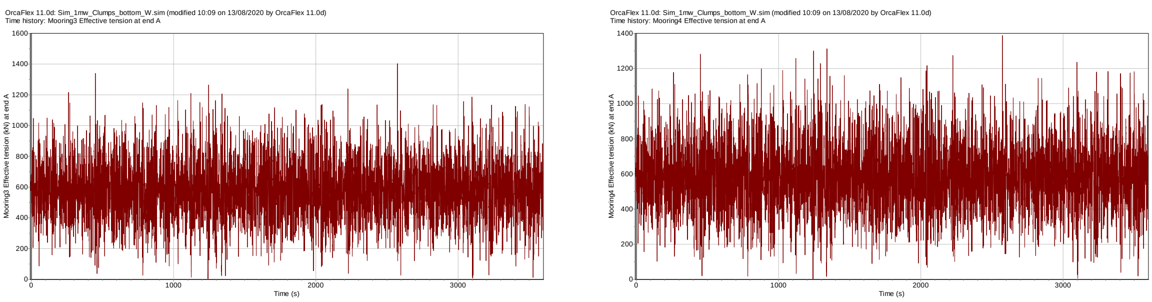


*Figure 7-6: ULS – Load Case 2 – Tension (kN) in (a) Mooring line 3 (b) Mooring Line 4*

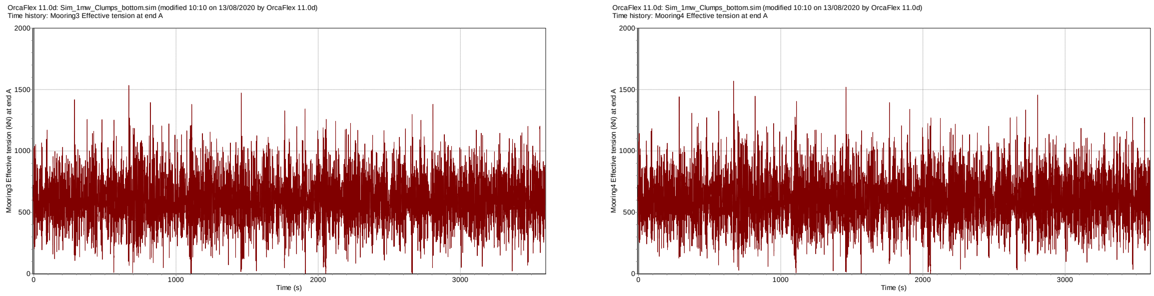


*Figure 7-7: ULS – Load Case 3 – Tension (kN) in (a) Mooring line 3 (b) Mooring Line 4*

The same explanations given for the base case are applicable for this case too. The slightly higher effective tension in line 3 than line 4 which is due to the yaw moment. It can be seen from the figures that worst case in the ULS is load case 1 since maximum effective tension has occurred in this case in line 3, i.e. 1688.35kN. Thus, for the ALS load case 1 is considered with line 3 as broken and the time series of the effective tension in line 4 is shown in Figure 7-8.

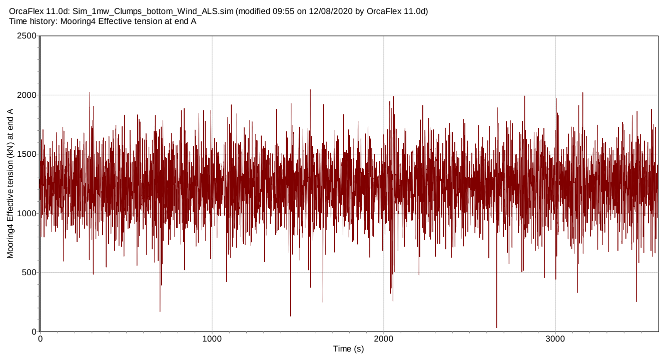


*Figure 7-8: ALS – Load Case 1 – Tension (kN) in Mooring line 4*

*Table 22: Hybrid Case: Summarised Result of Line 3*

| Limit State | Load Cases | Effective Tension at Line 3 (Platform End) | | | | Min Laying Length (m) | Effective Tension in Line 3 (Anchor End) | | | |
|---|---|---|---|---|---|---|---|---|---|---|
| | | Min (KN) | Max (KN) | Mean (KN) | Standard deviation (KN) | | Min (KN) | Max (KN) | Mean (KN) | Standard deviation (KN) |
| ULS | 1 | 0,51 | 1735,45 | 675,55 | 226,24 | 23,00 | -0,04 | 1688,35 | 635,92 | 212,33 |
| | 2 | 3,82 | 1403,46 | 583,23 | 185,31 | 23,00 | 0,00 | 1335,13 | 542,40 | 173,76 |
| | 3 | 0,67 | 1534,24 | 608,48 | 198,62 | 23,00 | -0,03 | 1471,63 | 566,74 | 186,08 |
| ALS | 1 | Broken | | | | | | | | |

*Table 23: Hybrid Case: Summarised Result of Line 4*

| Limit State | Load Cases | Effective Tension at Line 3 (Platform End) | | | | Min Laying Length (m) | Effective Tension in Line 3 (Anchor End) | | | |
|---|---|---|---|---|---|---|---|---|---|---|
| | | Min (KN) | Max (KN) | Mean (KN) | Standard deviation (KN) | | Min (KN) | Max (KN) | Mean (KN) | Standard deviation (KN) |
| ULS | 1 | -0,13 | 1.751,97 | 678,33 | 230,65 | 23,00 | 0,00 | 1.684,43 | 639,64 | 216,61 |
| | 2 | 1,39 | 1.388,14 | 585,43 | 188,16 | 23,00 | -0,04 | 1.325,22 | 547,22 | 176,70 |
| | 3 | 0,25 | 1.569,84 | 610,80 | 202,56 | 23,00 | 6,03 | 1.489,26 | 567,39 | 189,93 |
| ALS | 1 | 31,32 | 2.047,58 | 1.238,81 | 223,37 | 17,00 | 63,18 | 2.008,15 | 1.233,45 | 212,97 |

From the above tables, it can be inferred that the peak and mean tension is maximum for the load case 1 for the ULS which has had the highest wind speed. It has the same reason which was discussed for the base case due to the wind forces on the panel. For this case too, it will be interesting to study the fatigue loads on the line. The drag due to the current load is higher than the second-order wave loads as can be seen by the higher mean tension in load case 2 compared to 3. The above table also shows the information about the laying length and it is long enough for both limit state as well as the maximum tension generated for limit state, i.e. ULS and ALS are under the allowable breaking limit given in Table 12 (ULS-1884.46 kN and ALS-2517.64 kN) which justifies the reasonability of the choice of the chain size.

Table 24 and Table 25 shows the maximum amplitude from the mean position and the maximum acceleration of the extreme floaters respectively to provide motion of the full plant.

*Table 24: Hybrid Case: Maximum Amplitude from Mean Position*

| ULS – Load Case 1 | | | | |
|---|---|---|---|---|
| Floater No. | Maximum Amplitude from Mean Position | | | |
| | Surge (m) | Sway (m) | Pitch (deg) | Yaw (deg) |
| **1** | 0,45 | 8,71 | 4,94 | 1,07 |
| **4** | 0,63 | 8,75 | 4,75 | 1,04 |
| **13** | 0,51 | 9,10 | 4,82 | 0,84 |
| **16** | 0,56 | 8,99 | 4,04 | 0,96 |

| ULS – Load Case 2 | | | | |
|---|---|---|---|---|
| Floater No. | Maximum Amplitude from Mean Position | | | |
| | Surge (m) | Sway (m) | Pitch (deg) | Yaw (deg) |
| **1** | 0,69 | 8,63 | 4,76 | 1,14 |
| **4** | 0,86 | 8,60 | 4,99 | 1,10 |
| **13** | 0,64 | 8,47 | 4,16 | 0,86 |
| **16** | 0,72 | 8,45 | 4,65 | 0,78 |

| ULS – Load Case 3 | | | | |
|---|---|---|---|---|
| Floater No. | Maximum Amplitude from Mean Position | | | |
| | Surge (m) | Sway (m) | Pitch (deg) | Yaw (deg) |
| **1** | 0,45 | 8,65 | 4,39 | 1,16 |
| **4** | 0,54 | 8,67 | 4,60 | 1,19 |

| ALS – Load Case 1 | | | | |
|---|---|---|---|---|
| Floater No. | Maximum Amplitude from Mean Position | | | |
| | Surge (m) | Sway (m) | Pitch (deg) | Yaw (deg) |
| **1** | 7,04 | 21,60 | 4,95 | 10,15 |
| **4** | 8,21 | 8,60 | 7,77 | 9,57 |

| | | | | |
|---|---|---|---|---|
| **13** | 0,42 | 8,71 | 4,62 | 0,81 |
| **16** | 0,49 | 8,62 | 4,15 | 0,85 |

| | | | | |
|---|---|---|---|---|
| **13** | 7,48 | 19,62 | 10,40 | 9,83 |
| **16** | 6,35 | 8,13 | 4,98 | 10,30 |

It can be seen that the dominating motion of the plant is in sway motion and the maximum amplitude from the mean position and acceleration is observed of about 9m and 7m/s$^2$ respectively for the load case 1 in the ULS. While in the ALS the floater in the side at which the line is broken will have maximum motion, amplitude and acceleration of about 21 m. Here also in the ULS case, it can be seen that the motions in the load case 2 is higher than the load case 3, it is due to the dynamic loading of the wave on the floater.

*Table 25: Hybrid Case: Maximum Acceleration*

| **ULS - Load Case 1** | | | | |
|---|---|---|---|---|
| **Floater No.** | **Maximum Acceleration** | | | |
| | **Surge (m/s$^2$)** | **Sway (m/s$^2$)** | **Pitch (rad/s$^2$)** | **Yaw (rad/s$^2$)** |
| **1** | 2.90 | 7.06 | 1.14 | 0.20 |
| **4** | 2.31 | 6.42 | 0.85 | 0.37 |
| **13** | 1.68 | 5.66 | 0.71 | 0.35 |
| **16** | 2.05 | 6.29 | 0.62 | 0.44 |

| **ULS - Load Case 2** | | | | |
|---|---|---|---|---|
| **Floater No.** | **Maximum Acceleration** | | | |
| | **Surge (m/s$^2$)** | **Sway (m/s$^2$)** | **Pitch (rad/s$^2$)** | **Yaw (rad/s2)** |
| **1** | 2.63 | 5.13 | 1.00 | 0.16 |
| **4** | 2.67 | 4.25 | 0.54 | 0.39 |
| **13** | 1.36 | 4.52 | 0.50 | 0.23 |
| **16** | 1.85 | 4.76 | 0.94 | 0.22 |

| **ULS - Load Case 3** | | | | |
|---|---|---|---|---|
| **Floater No.** | **Maximum Acceleration** | | | |
| | **Surge (m/s$^2$)** | **Sway (m/s$^2$)** | **Pitch (rad/s$^2$)** | **Yaw (rad/s2)** |
| **1** | 2.44 | 6.23 | 1.04 | 0.32 |
| **4** | 2.28 | 5.25 | 0.61 | 0.29 |
| **13** | 2.28 | 5.13 | 0.78 | 0.35 |
| **16** | 2.12 | 6.15 | 0.71 | 0.35 |

It can be seen that the forces and the motions are slightly higher while using the hybrid mooring layout compared to the base layout. It was expected as the line length has reduced by a huge margin of 316m and because of it, the restoring force has also reduced. Whereas restoring force, in this case, is provided by the clumps. The difference like this is justifiable and accepted.

# 8. ANCHORS

Anchors are one of the major components in the mooring system as it maintains the station keeping of the system. It also has a major contribution to the cost of the mooring system as the installation procedure can be complex and expensive with some type of anchors. The size and selection of the type of anchor are depended upon three main factors load capacity, angle of load and ground condition.

For this thesis, drag anchor is selected for the station keeping as they are cheapest (cost + installation) as well as easiest to install. They can take up the horizontal load easily and a little bit of vertical loads which makes it ones of the most reliable and cheaper option for the catenary mooring. It is also suitable with the catenary as it doesn't require precise placement. Other options can be a possibility studied with different mooring layout that can further reduce the mooring footprint but it will make the system costlier. Therefore, it will be interesting to study another cycle of optimization between the mooring footprint and cost of the mooring system in the final stage.

Presently, the global soil condition of HKN which made up of sand is considered in the initial design, given in Table 9 but later on local condition of the soil where the plant is planned to be installed has to be taken. The factor of safety for the anchors, defined in Eq. (15) is also considered from the FOWT rules, taken from (BV - NI 572, 2019). The considered value for the ULS is 1.5 and for the ALS is 1.05.

$$SF = \frac{MHP}{Ta_{seabed}} \tag{15}$$

Where, MHP is the maximum holding power and $Ta_{seabed}$ is tangent-to-the-seabed component of the tension in line at the anchoring point when the design tension is applied to the fairlead.

Vryhof Stevin Mk3 anchor is selected for the choice of the drag anchors. A holding capacity versus weight diagram, shown in Figure 8-1 and the detail equation of it given in Table 26, is used to specify the size of the drag anchor needed.

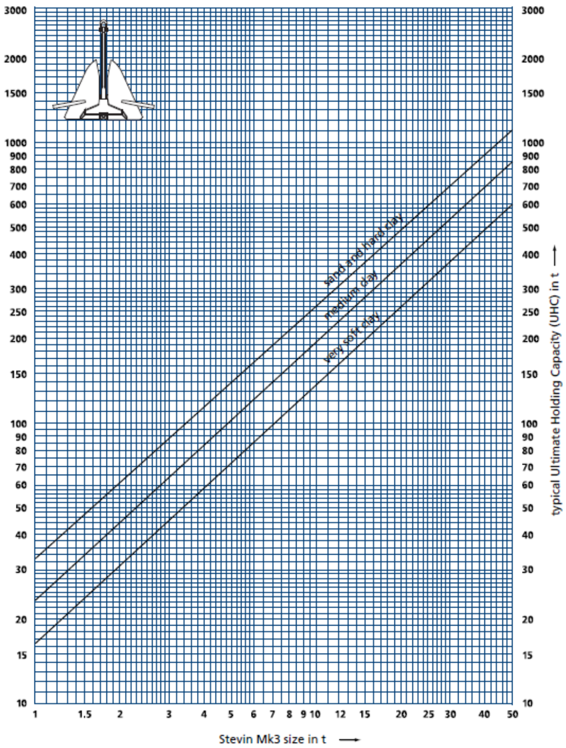


*Figure 8-1: Sizing Graph for Drag Anchor (Vryhof Anchors, 2010)*

*Table 26: Design Equations for Vryhof Stevin Mk3 Drag Anchors (ABS, 2013)*

| Soil | $UHC = a \times W^b$ • UHC: Anchor Ultimate Holding Capacity (kN) • W: Anchor Weight (MT) (1-50 MT) | |
|---|---|---|
| | **A** | **b** |
| **Very Soft Clay** | 161,23 | 0,92 |
| **Medium Clay** | 229,19 | 0,92 |
| **Sand and Hard Clay** | 324,42 | 0,9 |

Considering the maximum tensions at the anchor from the dynamic mooring analysis for both cases, the size of the anchor is calculated by the above graph. The results are summarised in Table 27.

*Table 27: Anchor Result*

| | **Sand and Hard Clay** | |
|---|---|---|
| | **Base Case** | **Hybrid Case** |
| **Anchor Weight (t)** | 9 | 10 |
| **UHC (kN)** | 2344 | 2577 |

# 9. CONCLUSION

Through this research thesis, a new design has been proposed for the floaters of FSPV plant for the offshore environment condition and also the mooring layout for it. It provides a good starting point for further research into the detail design of it. Since it is only looked with respect to the floater other aspects of the plant has to be studied.

The different design basis for the floater and the mooring system has been set up during this thesis, based on it their designs are done.

Diffraction analysis of a floater has been performed to study the hydrodynamic properties of the floater, later on, the diffraction analysis is done for the full plant to obtain the hydrodynamic data of the plant. Using this data dynamic mooring analysis is performed in the OrcaFlex for the base case and hybrid case. And an optimised version of mooring layout is proposed.

Finally, the anchor size is calculated for both mooring layouts.

Fatigue analysis was also performed but due to lack of time, the simulation was not completed. Therefore, its theory and data is not been included in the thesis.

# 10.FUTURE WORK

This thesis is a starting point in designing a new concept of the floating solar PV for the offshore condition. There is a long path of research of work that has to be done for the success of this design. Therefore, the pathway to succeed this task and become a pioneer in this domain is provided following a set of researches which has to be done in future.

- Fatigue analysis to get an idea
- Feasibility study of electrical cables and equipment
- Structural assessment and analysis
- Design of articulation
- Optimisation of solar modules
- CFD simulation of the wind loads on the panels
- CFD simulation for the drag coefficients on the floaters
- Optimization of mooring lines and fatigue analysis
- Model Testing
- Full-Scale Testing

# REFERENCES


ABS FOWTI, 2013. Guide for building and classing Floating Offshore Wind Turbine Installations.

Agarwal, A., Irtaza, H., Zameel, A., 2017. Numerical study of lift and drag coefficients on a ground-mounted photo-voltaic solar panel. Materialstoday: Proceedings 4, 9822–9827.

Ansys, 2017. Aqwa Theory Maual 18.2.

Browne, V.C., 2013. Assessment of Low-Frequency Roll Motions on the Semisubmersible Drilling Rig COSL Pioneer (Master thesis). Norwegian University of Science and Technology.

BV - NI 572, 2019. Classification and Certification of Floating Offshore Wind Turbines.

Chakrabarti, S.K., 2005. Handbook of Offshore Engineering. Nick Pinfield, Uk.

DHI, 2019. Metocean desk study and database Hollandse Kust (noord) Wind Farm Zone.

DNVGL-OS-E301, 2018. Offshore Standard - Position Mooring.

DNVGL-ST-0119, 2018. Standard - Floating wind turbine structures.

DNV-OS-J101, 2014. Offshore Standard - Design of Offshore Wind Turbine Structures.

DNV-RP-C205, 2010. Recommended Practice -Environmental Condition and Environmental Loads.

Fugro Survey B.V., 2018. Geophysical Survey - Hollandse Kust (noord) Wind Farm Zone.

Hole, K.B., 2018. Design of Mooring Systems for Large Floating Wind Turbines in Shallow Water (Master thesis). Norwegian University of Science and Technology.

Irtaza, H., Agarwal, A., 2018. CFD Simulation of Turbulent Wind Effect on an Array of Ground-Mounted Solar PV Panels. The Institution of Engineers (India) 99, 205–218.

Orcina, 2020. OrcaFlex Manual.

Rosa-Clot, M., Tina, G.M., 2020. Floating PV Plants. Brian Romer.

Wang, D., O'Loughlin, C.D., 2014. Numerical study of pull-out capacities of dynamically embedded plate anchors. Can. Geotech. J. 51, 1263–1272.

# APPENDIX A

The RAO’s value for 6 DOF for floaters of the FSPV Plant when the wave is coming from 0 degrees are shown in the graphs below:

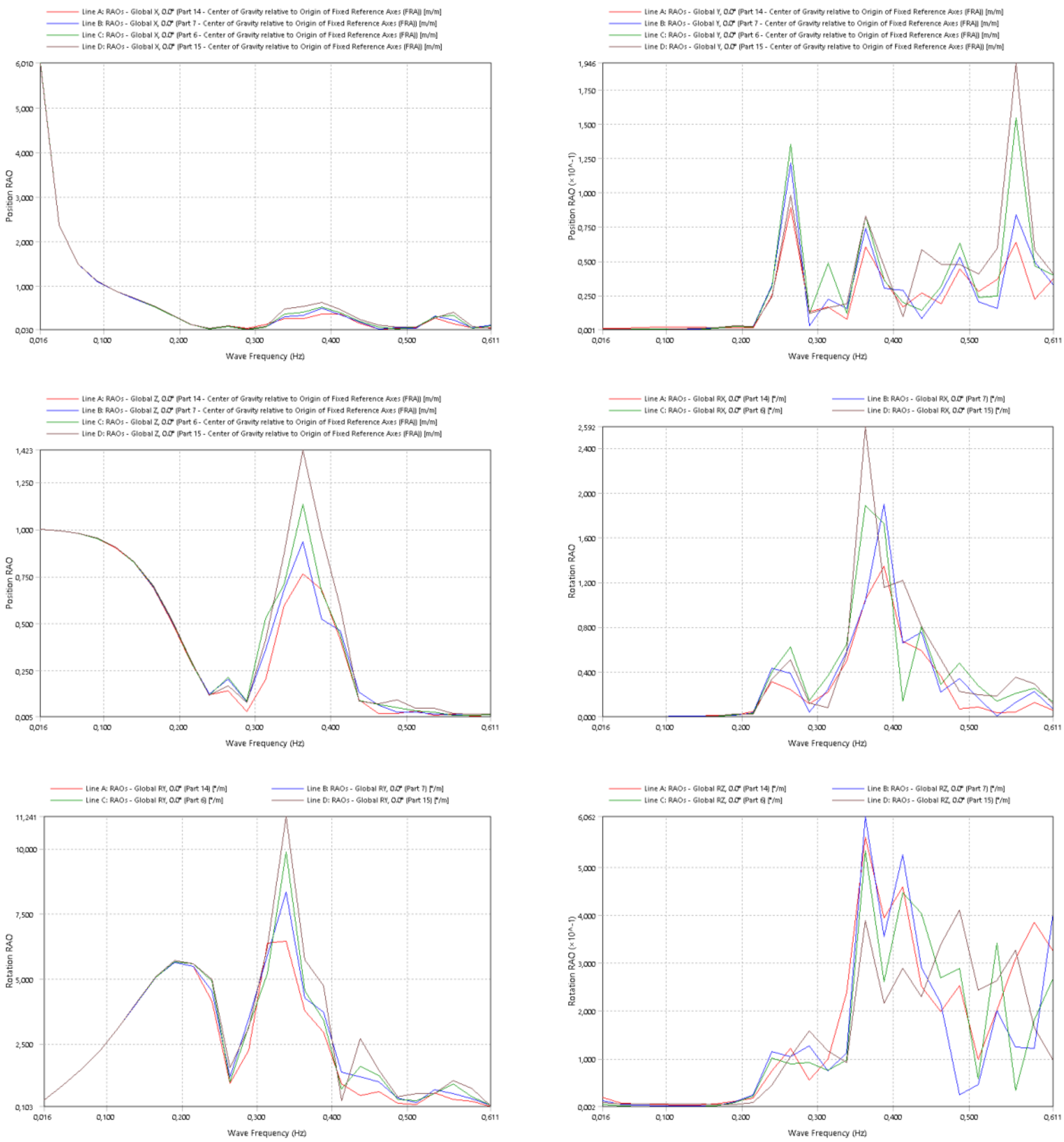


*Figure 0-1: RAO of a row of floaters of FSPV plant (a) Surge (b) Sway (c) Heave (d) Roll (e) Pitch (f) Yaw*